NR2F2 is required in the embryonic testis for Fetal Leydig Cell development

Aitana Perea-Gomez[1,*], Natividad Bellido-Carreras[1], Magali Dhellemmes[1], Furong Tang[1], Coralie Le Gallo[1], and Marie-Christine Chaboissier[1,*]

[1]Université Côte d'Azur, CNRS, INSERM, iBV, Nice, France

* Corresponding authors:
Aitana Perea-Gomez (Aitana.PEREA-GOMEZ@univ-cotedazur.fr)
Marie-Christine Chaboissier (Marie-Christine.CHABOISSIER@univ-cotedazur.fr)

Author Contributions: APG and MCC contributed to conception and design of the study. APG, NBC, FT, CLG and MD carried out experimental work. APG and MCC wrote the first draft of the manuscript. All authors contributed to manuscript revision, read, and approved the submitted version. Funding and Resources: MCC; Supervision: APG and MCC.

Competing Interest Statement: Authors declare that they have no competing interests.

Classification: Biological Sciences, Developmental Biology.

Keywords: NR2F2, Leydig, testis, mouse, embryo.

This PDF file includes:

Main Text
Figures 1 to 4
Figures S1 to S5
Tables S1 to S3

Abstract

Male genital development in XY mammalian fetuses is triggered by the action of hormones, including testosterone, secreted by the developing testes. Defects in this process are a cause for Differences in Sex Development (DSD), one of the most common congenital abnormalities in humans. Fetal Leydig Cells (FLC) play a central role for the synthesis of masculinizing hormones in the developing testes. Yet, the genetic cascade controlling their differentiation is poorly understood. Here we investigate the role of the orphan nuclear receptor NR2F2 in FLC development. We report that NR2F2 is expressed in interstitial progenitor cells of the mouse embryonic testes and is downregulated upon their differentiation into FLC. By using two mouse models for conditional mutation of *Nr2f2* in the developing testes we demonstrate that NR2F2 is required for testis morphogenesis and FLC development. NR2F2 acts in interstitial progenitors to regulate the initiation and progression of FLC differentiation independently of paracrine signaling pathways known to control this process. These results establish NR2F2 as an essential regulator of FLC development and steroid hormone synthesis in the mouse fetal testis and provide an entry point to understand the etiology of 46, XY DSD associated to pathogenic NR2F2 variants.

Main Text

Introduction

Sexual development in mammals is conditioned by the gonadal sex established during fetal life. In XY embryos, the initially undifferentiated gonads develop into testes that can produce testosterone which stimulates the growth of male internal and external genitalia (including epididymis, vas deferens, seminal vesicles, and penis) leading to the masculinization of the fetus. In contrast, fetal ovaries do not produce testosterone and female internal and external genitalia (oviducts, uterus, vagina, and vulva) develop in XX individuals. Abnormalities in the masculinization process are mainly associated with defects in the androgen synthesis or action (1). Although this molecular cascade is well defined, the differentiation of androgen-producing cells in the embryo is only partially understood.

Androgen production in the developing testis relies mainly on Fetal Leydig Cells (FLC), which express all enzymes required for the biosynthesis of androstenedione from cholesterol (2–5). The final step of conversion of androstenedione into testosterone, catalyzed by HSD17B3, takes place in a different cell type, the fetal Sertoli cells (4, 6). In addition to their role in androgen synthesis, FLC also produce INSL3, a hormone required for testis descent (7, 8). Defects in this process, regulated also by androgens, result in cryptorchidism, a condition which impacts fertility and constitutes a risk factor for testicular cancer (9). While a fraction of FLC persist after birth, others de-differentiate or involute so that testosterone production in adult life is ensured by a distinct population of steroidogenic cells, the Adult Leydig cells (ALC) that differentiate at puberty (10, 11).

FLC differentiate from embryonic day 12.5 (E12.5) in mice and increase in number during fetal life exclusively through the recruitment and differentiation of proliferative progenitors located in the interstitial space of the testes (10–12). Interstitial progenitors also give rise to the contractile peritubular myoid cells (PTM) that will surround the future seminiferous tubules (5). Despite being the most abundant cell population of the fetal testis (5, 13), little is known about the genetic control of interstitial steroidogenic progenitor proliferation, specification, and differentiation.

Lineage tracing and single cell transcriptomic analyses have revealed that interstitial progenitors have a dual origin. The majority are derived from the coelomic epithelium of the undifferentiated gonad which harbors early bipotential precursors able to differentiate along the supporting (the future Sertoli cells) or the steroidogenic lineage (5, 14–16). In addition, Nestin-positive cells migrate from the adjacent mesonephros into the gonad and differentiate along the steroidogenic lineage from E13.5 to give rise to up to a third of the FLC population at the end of gestation (5, 17, 18).

Interstitial progenitors differentiate in response to paracrine signals (12, 19). Desert Hedgehog (DHH) secreted by Sertoli cells acts on the interstitial progenitors expressing the Hedgehog receptor Patched1 (PTCH1) and the Hedgehog effectors GLI1, 2 and 3 to trigger FLC and PTM differentiation (20–26). In addition FLC development requires the activation of signaling pathways downstream of PDGFRA in the steroidogenic progenitors (27–29). On the other hand, ligands present in vascular and peri-vascular cells activate NOTCH2 receptor and the expression of the effectors HES1 and HEYL in interstitial progenitors to maintain their undifferentiated state and restrict FLC formation (18, 30–32). Paracrine signals acting on progenitors converge to regulate the transcription factors NR5A1, GATA4 and GATA6 which drive FLC differentiation by controlling the expression of genes related to cholesterol metabolism and steroidogenesis (33–39). In addition to the paracrine signals, interstitial steroidogenic progenitors differentiation along the

FLC lineage is also regulated by the cell-autonomous action of the transcription factors ARX, TCF21, PBX1, MAF and MAFB, although their precise roles remain elusive (5, 40–43).

NR2F2 is an orphan nuclear receptor that regulates tissue differentiation and homeostasis by activating or repressing transcription depending on the cellular context (44). *Nr2f2* mutation in mouse results in angiogenesis and heart development defects leading to embryonic lethality at mid-gestation (45). NR2F2 is expressed in interstitial progenitors of the fetal and adult testis in rodents and human (3, 5, 46–51). The study of mouse conditional mutants has established that NR2F2 is essential for ALC differentiation in the post-natal testis before puberty (50). However, the function of NR2F2 in the developing testis during fetal life has not been addressed and its role in the interstitial progenitors that give rise to the FLC lineage is currently unknown. It was initially proposed that NR2F2 could act as a negative regulator of steroidogenesis at fetal stages based on the inverse correlation between NR2F2 expression and steroidogenesis genes and testosterone levels in mouse and rat fetal testes treated with endocrine disruptors (48). More recently, rare variants in NR2F2 have been associated with cryptorchidism, hypospadias and defective penile growth in human patients (52, 53). These phenotypes can be attributed to defective testosterone and INSL3 production during gestation (9, 54), suggesting a positive role for NR2F2 in promoting FLC differentiation and/or function in the fetal testis.

In this study we show that NR2F2 is expressed in interstitial progenitors of coelomic and mesonephric origin of the mouse fetal testes and is downregulated upon FLC differentiation. By using two Cre lines that drive *Nr2f2* deletion in mouse embryonic gonads we show that NR2F2 is required for fetal testis morphogenesis and for FLC differentiation. *Nr2f2* mutation does not impair paracrine signals known to regulate FLC differentiation nor the proliferation or survival of the steroidogenic progenitor population. Our findings reveal that NR2F2 functions by promoting the initiation of FLC differentiation as well as FLC maturation. Together these results establish NR2F2 as an essential factor that positively regulates steroidogenic cell development in the mouse fetal testis.

Results

NR2F2 is expressed in steroidogenic progenitors of the developing testis

We examined the spatio-temporal distribution of NR2F2 in the developing testis by immunofluorescence. At E11.5 (18-21 tail somites, ts) NR2F2 was detected in both the coelomic epithelium and the mesonephric mesenchyme adjacent to the gonads, two tissues that contribute to the population of interstitial steroidogenic progenitors (5, 14, 18) (Fig. 1 *A* and *C*). The majority of mesenchymal cells in the gonad expressed the transcription factor RUNX1 (55), indicating that most of the gonadal somatic cells at this stage belong to the supporting lineage (Fig. 1 *A* and *D*). Nevertheless, NR2F2+ RUNX1- cells were observed, revealing that interstitial progenitors were already present at this stage (Fig. 1*A*). NR2F2+ cells were either GATA4+ or GATA4-, suggesting that interstitial progenitors of coelomic and mesonephric origins respectively, were both present (Fig. 1 *A*-*C*).

In E12.5 testes, NR2F2 positive cells were detected in the coelomic epithelium and in the interstitial space outside the developing testis cords (Fig. 1 *E*-*H*, Fig. S1 *A*-*D*). NR2F2 positive cells co-expressed the steroidogenic progenitor marker ARX (5, 40), and were actively proliferating (Fig.1 *E*-*H*, Fig. S1 *E*-*H*). At E14.5, NR2F2 expression was maintained in interstitial cells co-expressing PDGFRA (27), as well as in the peritubular myoid cells lining the testis cords and in the cells beneath the surface of the testis that will contribute to the future tunica albuginea (Fig. 1 *I* and *J*, Fig. S1 *M*-*P*). NR2F2 expression was also found in NESTIN expressing peri-vascular cells that correspond to the mesonephros derived steroidogenic progenitors (18) (Fig. 1 *K* and *L*). In contrast,

NR2F2 protein was either absent or detected at very low levels in FLC marked by the expression of the steroidogenic enzyme HSD3B (Fig. 1 *M-P*, Fig. S1 *I-L*).

Together our results demonstrate that NR2F2 is expressed in the coelomic epithelium and the mesonephros as well as in the interstitial progenitors derived from the two sources and is downregulated upon FLC differentiation in the developing testis.

NR2F2 is required for fetal testicular morphogenesis and FLC development

In order to investigate the function of NR2F2 in the developing mouse testis, we used a *Nr2f2*^{flox} conditional allele (9), and a knock-in *WT1*^{CreERT2} line, in which tamoxifen inducible CreERT2 is produced by WT1 expressing cells (10). *Wt1* is expressed from E9.5 in the coelomic epithelium of the gonadal ridge and in the adjacent mesonephros (58) and WT1^{CreERT2} mediated recombination can be induced in all somatic gonadal cells upon tamoxifen administration at E9.5 and E10.5 (59) (Fig. S2*A*).

NR2F2 is co-expressed with WT1 in the gonadal coelomic epithelium, in the mesonephros and in interstitial cells (60)(Fig. S2 *C-F*). Tamoxifen treatment at E9.5 and E10.5 triggered an efficient NR2F2 deletion in gonadal and mesonephric tissues of *WT1*^{CreERT2}*; Nr2f2*$^{flox/flox}$ embryos examined at E12.5 and E14.5 (Fig. 2 *A-D*, Fig. S2*B*). NR2F2 expression was completely absent in gonadal interstitial cells including NESTIN+ cells, demonstrating that all interstitial steroidogenic progenitors were targeted in *WT1*^{CreERT2}*; Nr2f2*$^{flox/flox}$ embryos (Fig. 2 *C* and *D*). Morphological examination of the urogenital system of E16.5 *WT1*^{CreERT2}*; Nr2f2*$^{flox/flox}$ embryos revealed hypoplastic undescended testes (Fig. S2 *G* and *H*), indicating that NR2F2 function is required for testicular development.

The initial specification of the supporting and steroidogenic lineages occurred in absence of NR2F2 as shown by the presence of Sertoli cells expressing SOX9 (Fig. 2 *A* and *B*) and interstitial progenitors marked by ARX (Fig. 2 *E* and *F)* in *WT1*^{CreERT2}*; Nr2f2*$^{flox/flox}$ embryos at E12.5. However, the mutant gonads exhibited almost a complete absence of differentiated steroidogenic FLC (marked by HSD3B expression) compared to controls (Fig. 2 *G*, *H* and *M*). This phenotype was not due to a delay in the initiation of FLC differentiation, as the number of HSD3B positive cells remained strongly reduced in *WT1*^{CreERT2}*; Nr2f2*$^{flox/flox}$ mutant gonads at E14.5 (60% reduction, Fig. 2 *K-M*). In addition, the transcripts of *Cyp11a1* and *Cyp17a1*, two genes encoding steroidogenic enzymes expressed in FLC, and of *Insl3* were strongly reduced (Fig. S2*K*). At E14.5, the mutant gonads showed enlarged and irregular shaped testis cords (Fig. 2*D*, Fig. S2*J*). Moreover, the expression of ACTA2 was strongly reduced at E14.5 both in the periphery of the gonad and in cells lining the testis cords, indicating that tunica cell and peritubular myoid cell development were impaired in *WT1*^{CreERT2}*; Nr2f2*$^{flox/flox}$ mutants (Fig. 2 *I* and *J*). Together these results demonstrate that NR2F2 function is not essential for the initial specification of the interstitial and supporting cells of the testis but is required for testicular morphogenesis and for FLC development.

Early *Nr2f2* deletion impairs Sertoli cell development

FLC differentiation relies on signals produced by Sertoli cells (12). Desert Hedgehog (DHH) secreted by Sertoli cells, activates its target genes such as *Gli1* in interstitial and promotes FLC differentiation (20, 21). PDGFA produced by Sertoli cells activates PDGFRA signaling required for FLC development (27, 29). The number of Sertoli cells expressing SOX9 was not altered in *WT1*^{CreERT2}*; Nr2f2*$^{flox/flox}$ mutants at E14.5 (Fig. 2*N*), however *Dhh* and *Pdgfa* transcript levels were lower in the *Nr2f2* mutant testes (Fig. 2*O*). Similarly, *Gli1* transcripts were reduced indicating that the activation of the Hedgehog pathway is impaired in *WT1*^{CreERT2}*; Nr2f2*$^{flox/flox}$ gonads (Fig. 2*O*, Fig. S2*L*). We found that the expression of *Amh*, another marker of differentiated Sertoli cells, was also reduced in the mutant compared to control gonads, while *Sox9* expression was unchanged (Fig. 2*O*, Fig. S2*L*). These observations indicate that Sertoli cell differentiation is abnormal in *WT1*^{CreERT2}*;*

Nr2f2$^{flox/flox}$ gonads. NR2F2 is co-expressed with WT1 in coelomic epithelium progenitors that will give rise to both supporting and steroidogenic lineages (Fig. S2 *C-F*, (5, 15)). We infer that tamoxifen induction at E9.5 and E10.5 drives early deletion of NR2F2 in coelomic epithelium progenitors of *WT1*^{CreERT2}*; Nr2f2*$^{flox/flox}$ mutants leading to deficient differentiation of supporting cells, reduced production of DHH and PDGFA and impaired FLC development.

NR2F2 is required in the steroidogenic lineage for FLC development

In order to elucidate the specific function of NR2F2 in the steroidogenic lineage for FLC development we used the transgenic *Nr5a1-Cre* line which drives robust recombination in somatic gonadal cells from E11.5, after the supporting and steroidogenic lineages have been specified (Fig. S3 *A* and *B*)(61, 62).

At E11.5, NR5A1 is co-expressed with NR2F2 in the gonadal coelomic epithelium and in interstitial cells, but is absent from the mesonephros and mesonephros derived cells (15, 18)(Fig. S3 *D-G*). *Nr5a1-Cre; Nr2f2*$^{flox/flox}$ mutants show efficient NR2F2 deletion in gonadal interstitial cells at E12.5 and E14.5 (Fig. 3 *A-D*, S3*C*). Consistent with previous reports on the activity of *Nr5a1-Cre* (62), NR2F2 was still detected in the coelomic epithelium layer and in interstitial cells just beneath it, particularly in the anterior part of the gonad of *Nr5a1-Cre; Nr2f2*$^{flox/flox}$ mutants (Fig. 3 *A-D*). NESTIN+ NR2F2+ cells were still present, confirming that steroidogenic progenitors of mesonephric origin were not targeted by *Nr5a1-Cre* (Fig. 3 *C* and *D*)(18). Together these results demonstrate that in *Nr5a1-Cre; Nr2f2*$^{flox/flox}$ mutants, NR2F2 is deleted after E11.5 in interstitial cells derived from the coelomic epithelium except in the outermost layer of the testis.

Nr2f2 deletion by *Nr5a1-Cre* did not affect the initial formation of the supporting and steroidogenic lineages as evidenced by SOX9 (Fig. 3 *A* and *B*, Fig. S3*L*) and ARX expression (Fig. 3 *E* and *F*), nor the differentiation of Sertoli cells as shown by normal expression levels of *Dhh, Pdgfa* and *Amh* (Fig. 3*G*, Fig. S3*M*). In addition, ACTA2 was detected in peritubular myoid cells and was only slightly reduced in the tunica albuginea of the posterior region in the mutant testes (Fig. S3 *H* and *I*). In contrast, the FLC population marked by HSD3B or CYP11A1 was decreased (40% reduction, Fig. 3 *H-L*, Fig. S3 *J* and *K*) and the expression of the FLC markers *Cyp11a1*, *Cyp17a1* and *Insl3* was strongly down-regulated in *Nr5a1-Cre; Nr2f2*$^{flox/flox}$ mutant testes (Fig. 3*M*). In agreement with reduced FLC function during embryogenesis, the testis of *Nr5a1-Cre; Nr2f2*$^{flox/flox}$ embryos were undescended and exhibited an abnormal abdominal position at postnatal day (P) 3 (Fig. 3 *N* and *O*).

We conclude that *Nr2f2* deletion after E11.5 by *Nr5a1-Cre* leads to FLC reduction without Sertoli cell defects suggesting that NR2F2 is required cell-autonomously in the interstitial cells for FLC development.

NR2F2 acts independently of DHH, PDGFRA and NOTCH pathways in FLC differentiation

We next investigated the impact of *Nr5a1-Cre; Nr2f2* $^{flox/flox}$ mutation on the signaling pathways involved in FLC differentiation. *Dhh* and *Gli1* expression, a readout of Hedgehog pathway activation, were not modified in *Nr5a1-Cre; Nr2f2*$^{flox/flox}$ mutants (Fig. 3*G*, Fig. S3*M,* Fig. *S4A*). The expression of *Pdgfa* and *Pdgfb*, coding for two PDGFRA ligands expressed in developing testes (27), of *Pdgfra* and of *Sgpl1*, a PDGFRA signaling target involved in steroidogenic differentiation (29), were not altered in *Nr5a1-Cre; Nr2f2*$^{flox/flox}$ mutants (Fig. 3*G*, Fig. S4*A*). We conclude that Hedgehog and PDGFRA signaling, two pathways required for FLC differentiation, are not impaired in *Nr5a1-Cre; Nr2f2*$^{flox/flox}$ mutants.

In addition to the positive signals mediated by DHH and PDGFRA, FLC differentiation is also negatively modulated by NOTCH signaling triggered by ligands expressed in vascular and peri-vascular cells (18, 30–32). The receptor NOTCH2 expressed in interstitial cells is involved in restricting FLC differentiation (18, 30–32). *Notch2* mRNA levels were not altered in *Nr5a1-Cre;*

Nr2f2$^{flox/flox}$ mutants (Fig. S4*A*). NOTCH signaling activates the expression of its target genes that also act as effectors of the pathway including *Heyl*, specifically expressed in interstitial cells and strongly up-regulated upon vascular depletion (18) and *Hes1,* expressed in interstitial cells and involved in restricting FLC differentiation (30, 31). *Hes1*, *Heyl* and *Cdh5* transcripts (a readout of the abundance of endothelial cells) were detected at similar levels in controls and *Nr5a1-Cre; Nr2f2*$^{flox/flox}$ mutants (Fig. S4*A*), indicating that the observed decrease in FLC numbers cannot be attributed to an increase in vascular cells associated to excessive NOTCH signaling.

Together these results indicate that NR2F2 deficiency does not impact the signaling pathways that are known to induce or repress FLC formation. This suggests that NR2F2 acts downstream or in parallel of these pathways during the process of FLC differentiation.

NR2F2 promotes the initiation of FLC differentiation and FLC maturation

FLC differentiate from proliferating interstitial progenitors that progressively lose their mitotic ability, downregulate the transcription factors ARX and NR2F2, up-regulate the master regulator of steroidogenesis NR5A1 and activate the expression of steroidogenesis related genes (3, 5, 40). This differentiation process is accompanied by a change in cell shape from spindle shaped progenitors to round shaped FLC, and an increase in cytoplasmic volume (48, 63). We wanted to determine which of these steps of FLC differentiation are NR2F2 dependent.

The transcription factor ARX is required in the pool of proliferating interstitial progenitors for FLC development (40). We first examined whether NR2F2 regulates the survival, proliferation or identity of the ARX+ cell population. We found that the expression of *Arx* mRNA was not modified in *Nr5a1-Cre; Nr2f2*$^{flox/flox}$ mutants (Fig. S4 *A* and *D*). The percentage of ARX+ cells among the total number of gonadal cells and the fraction of proliferating cells among the ARX+ population were similar to controls at E12.5 and E14.5 (Fig. 4 *A, B* and *E*, Fig. S4 *B-D*). In addition, we did not find evidence of increased cell death in *Nr5a1-Cre; Nr2f2*$^{flox/flox}$ mutants (Fig. S4 *E-G).* Together these results indicate that ARX+ steroidogenic progenitor cells are present and proliferate at normal rates in *Nr5a1-Cre; Nr2f2*$^{flox/flox}$ mutants.

As the ARX+ steroidogenic progenitors adopt a FLC identity, NR2F2 is progressively lost and the nuclear receptor NR5A1 is strongly up-regulated (3, 5, 48). NR5A1 directs FLC differentiation by regulating the expression of genes associated to cholesterol metabolism and steroidogenesis (33, 36, 64, 65). In *Nr5a1-Cre; Nr2f2*$^{flox/flox}$ mutants the number of cells expressing high levels of NR5A1+ in the interstitial compartment was reduced compared to controls (Fig. 4 *C-E*). This observation indicates that NR2F2 function is required for the initial step of steroidogenic cell differentiation at the time of NR5A1 up-regulation.

A small fraction of FLC formed in absence of NR2F2 function, even in the case of *WT1*^{CreERT2}*; Nr2f2*$^{flox/flox}$ mutant gonads that exhibit widespread NR2F2 deletion in steroidogenic progenitors of coelomic and mesonephric origin. To evaluate the steroidogenic capacities of FLC in the *Nr2f2* mutant gonads, we analyzed the transcript levels of *Star,* encoding the steroidogenic acute regulatory protein involved in cholesterol transport, *Cyp11a1* and *Cyp17a1* normalized to the FLC number as quantified by HSD3B immunofluorescence (Fig. 2*M,* Fig. 3*L*) (24). Normalized data showed reduced steroidogenic gene expression in *Nr5a1-Cre; Nr2f2*$^{flox/flox}$ and in *WT1*^{CreERT2}*; Nr2f2*$^{flox/flox}$ mutant testes (Fig. 4*F*, Fig. S5*E*), suggesting that FLC formed in the mutant testes have reduced steroidogenic function. In addition, HSD3B positive FLC present in *Nr5a1-Cre; Nr2f2*$^{flox/flox}$ and in *WT1*^{CreERT2}*; Nr2f2*$^{flox/flox}$ mutants were smaller and more elongated than those in control littermates (Fig. 4 *G-I*, Fig. S4*H*, Fig. S5 *A-D*). These cellular characteristics have been associated to immature FLC at the initial stages of FLC differentiation before the formation of large and round testosterone producing FLC (48, 63).

Taken together, our results show that NR2F2 is required in interstitial steroidogenic progenitor cells for the up-regulation of NR5A1 and the initiation of FLC differentiation but also for the subsequent step of FLC maturation leading to robust steroid production.

Discussion

NR2F2 protein is expressed in interstitial cells of coelomic epithelium and mesonephric origin and is absent or detected at very low levels in FLC as soon as they are formed at E12.5. Our observations are consistent with NR2F2 positive cells being progenitors for FLC (3, 5) and indicate that NR2F2 is quickly down-regulated upon differentiation of the fetal steroidogenic lineage, when the cells begin to synthetize steroid hormones.

We used two Cre lines to address the role of NR2F2 in the mouse fetal testis. In both cases *Nr2f2* mutants exhibit reduced FLC numbers, decreased steroidogenic gene expression and undescended testes. These findings identify NR2F2 as a positive regulator of FLC development in the mouse fetal testis. *Nr2f2* mutation does not impair the survival or proliferation of the interstitial steroidogenic progenitor population, nor the paracrine signals involved in FLC differentiation. We conclude that NR2F2 acts in steroidogenic progenitors as a permissive factor for the initiation of their differentiation into FLC. NR5A1 is a master regulator of steroidogenic differentiation essential for FLC differentiation (33–36). Failure to up-regulate NR5A1 in a fraction of FLC in *Nr2f2* mutants is sufficient to account for the decrease in FLC numbers. Future work will aim at determining whether NR2F2 regulates NR5A1 expression directly or indirectly.

In contrast to the situation in *Nr5a1* mutants where FLC are completely absent (36), a fraction of FLC differentiates in *Nr2f2* mutants even when progenitors of both coelomic epithelium and mesonephric origin are targeted. This observation indicates that additional factors cooperate with NR2F2 to regulate the transition from the steroidogenic progenitor state to the differentiating FLC. The homeodomain protein ARX is expressed in *Nr2f2* mutant steroidogenic progenitors and is a good candidate to be such a factor. *Arx* mutants exhibit decreased FLC numbers without defects in paracrine signals driving their differentiation, similar to *Nr2f2* mutants (40).

FLC and ALC are morphologically, transcriptionally and functionally distinct (11, 66), yet NR2F2 function is required for the differentiation of both lineages. In contrast to the situation in the fetal testis, NR2F2 is maintained in cells that have started to express steroidogenesis genes in the post-natal testis (3, 5, 46). NR2F2 regulates the transition from the adult progenitor Leydig cell (characterized by their elongated shape, their ability to proliferate and a low level of testosterone synthesis) to the immature ALC (characterized by their round shape, low mitotic activity and increased testosterone production) (50, 63). In agreement with its *in vivo* role promoting maturation along the ALC lineage, NR2F2 co-operates with NR5A1 and GATA4 to activate the transcription of *Insl3*, *Star* (encoding the cholesterol transporter) and *Amhr2* (46, 67–70) in MA-10 cells, an *in vitro* model for immature ALC. Here we found that the steroidogenic cells that differentiate in *Nr2f2* mutant fetal testes exhibit a small size, an elongated shape and reduced steroidogenic gene expression, features of the earliest stages of FLC differentiation (19, 48, 63). A similar phenotype is obtained when *Nr5a1* is deleted after the onset of FLC differentiation (65). This suggests that in addition to controlling the initial engagement of steroidogenic progenitors into the FLC lineage and similar to the situation in the post-natal testis, NR2F2 promotes FLC maturation possibly by regulating the expression of genes involved in steroidogenesis.

NR2F2 is required for additional aspects of fetal testis morphogenesis and differentiation. Testis cords are enlarged and abnormally shaped in *Nr2f2* mutants. Testis cord development involves the formation of Sertoli-germ cell masses after E11.5 and their subsequent partition by growing wedges of interstitial cells and associated vascular branches at E12.5 (71). How NR2F2 dependent regulation of interstitial cell adhesion or migration contributes to this process will be the

aim of future research. Sertoli cell differentiation is specifically impaired in *WT1*^{CreERT2}*; Nr2f2*$^{flox/flox}$ mutants. We hypothesize that *WT1*^{CreERT2} induction at E9.5 and E10.5 triggers an early deletion of NR2F2 in the bipotential progenitors that impacts Sertoli cell differentiation, a defect that might be exacerbated due to the heterozygosity for WT1 in these animals. The *WT1*^{CreERT2} line also targets the outermost interstitial cells of the testis, revealing a function of NR2F2 in the cells that will form the tunica albuginea.

Pathogenic variants in NR2F2 have been associated with congenital malformations including congenital heart disease, congenital diaphragmatic hernia and syndromic 46,XX testicular or ovo-testicular difference/disorder in sex development (DSD) (44, 72). More recently, defects in the external genitalia (micropenis, hypospadias), and cryptorchidism have been associated to rare heterozygous variants in NR2F2 in 46, XY patients (52, 53). These phenotypes can be attributed to defects in testosterone-dependent masculinization and INSL3-dependent testis descent during gestation and could be explained by a failure of FLC differentiation in the fetal testis. NR2F2 is abundantly expressed in interstitial cells of fetal human testes, a population that likely contains the progenitors for FLC (47–49, 51). The present work demonstrating that NR2F2 is required in the steroidogenic progenitors of the murine fetal testis for the initiation and progression of FLC differentiation provides an entry point to understand the etiology of 46, XY DSD associated to pathogenic NR2F2 variants.

Materials and Methods

Mouse Strains and Genotyping

The experiments described herein were carried out in compliance with the relevant institutional and French animal welfare laws, guidelines and policies. Mouse lines were kept on a mixed background B6CBAF1/JRj. The *Nr2f2*^{tm1Vc} line where *Nr2f2* exon1 sequences (encoding the DNA binding domain) are deleted upon CRE mediated recombination (referred to as *Nr2f2*^{flox}), the knock-in *Wt1*$^{tm2(cre/ERT2)Wtp}$ line where tamoxifen inducible Cre^{ERT2} is produced by WT1 expressing cells (referred to as *WT1*^{CreERT2}), and the transgenic *Tg(Nr5a1-cre)2Klp* line where Cre expression is driven by *Nr5a1* regulatory sequences (referred to as *Nr5a1-Cre*), were genotyped as previously described (56, 57, 61). *WT1*^{CreERT2}*; Nr2f2*$^{flox/+}$ or *Nr5a1-Cre*$^{tg/0}$*; Nr2f2*$^{flox/+}$ males were crossed with *Nr2f2*$^{flox/+}$ females to obtain mutant embryos at different stages. Embryos were named controls (*Nr2f2*$^{+/+}$ or *Nr2f2*$^{flox/+}$) or mutants (*WT1*^{CreERT2}*; Nr2f2*$^{flox/flox}$ or *Nr5a1-Cre*$^{tg/0}$*; Nr2f2*$^{flox/flox}$). Genotypes of mice and embryos were determined using PCR assays on lysates from ear biopsies or tail tips. Genotyping primers are listed in Table S1. To activate the Cre^{ERT2} recombinase in embryos, tamoxifen (TAM, T5648, Sigma-Aldrich) was directly diluted in corn oil to a concentration of 40 mg/mL, and two TAM treatments (200 mg/kg body weight) were administrated to pregnant females by oral gavage at E9.5 and E10.5. For proliferation assays, 5-Bromo-2'-deoxy-Uridine (BrdU) (B5002, Sigma-Aldrich) was diluted to a concentration of 10 mg/mL in sterile H_2O, was administrated to the pregnant females (50 mg/kg body weight) by intraperitoneal injection, and pregnant females and their embryos were humanely killed after 3 hours and 30 min. The day when a vaginal plug was found was designated as embryonic day E0.5. E11.5–E12.5 embryos were staged by counting the number of tail somites (ts) with 18 ts corresponding to E11.5.

Immunofluorescence staining

Embryos were fixed in 4% (*w/v*) paraformaldehyde (PFA, 15710-S, EMS) overnight, processed for paraffin embedding, and sectioned into 5 µm thick sections. Immunofluorescence and DAPI staining were performed as described in (73). Proliferation analysis was performed by using a BrdU detection kit (11 296 736 001, Roche). Images were obtained on a motorized Axio

Imager Z1 microscope (Zeiss) coupled with an AxioCam MRm camera (Zeiss) and processed with Fiji (Bethesda, MD, USA). The DAPI staining marking the nuclei was adjusted to visualize the tissues and may vary between samples. However, for the immunofluorescence analysis, the exposure time of the acquisition of the fluorescent signal was identical in the same experiment to allow comparison between controls and mutants. Images were assembled using the open-source software platform OMERO (https://www.openmicroscopy.org/omero/). Antibodies are listed in Table S2. At least three embryos of each genotype were analyzed for each marker.

Cell Quantifications

The gonadal area for each section was measured by creating a gonadal Region of Interest (ROI) drawn manually in Fiji. The number of HSD3B positive cells, SOX9 positive cells, NR5A1 positive cells, ARX positive cells, ARX positive cells that had incorporated BrdU, Activated Caspase 3 positive cells or the number of nuclei labelled by DAPI, were counted manually using the cell counter Plugin from Fiji. For each genotype, gonads of 3 or 4 biological replicates were analyzed. Two to three coronal sections spaced by at least 30 µm in the medial regions of the gonads were analyzed for each individual. Statistical significance was assessed by Mann-Whitney U two-tailed test. * indicates P value ≤ 0.05; ns indicates P value > 0.05.

Quantification of area and circularity of HSD3B positive cells

Gonadal (ROI) were drawn manually, and HSD3B positive cells were segmented using Stardist Deep Learning plugin of Fiji with a minimum area of 20 μm^2 to remove small particles. The area and circularity of each segmented cell were measured with Fiji. Circularity = 4π*area/perimeter^2. A value of 1.0 indicates a perfect circle. As the value approaches 0.0, it indicates an increasingly elongated shape. For each genotype, 2 to 3 biological replicates were analyzed. The data are shown as violin plots (with median and quartiles) for control and mutant samples.

RNA extraction and Quantitative PCR analysis

Individual gonads were dissected from the mesonephros in PBS, snap-frozen in liquid nitrogen and kept at −80 °C. RNA was extracted by RNeasy Micro Kit (74004, Qiagen) and reverse transcribed by M-MLV reverse transcriptase (M170A, Promega). The cDNA was used as a template for quantitative PCR analysis using the SYBR Green I Master (04887352001, Roche) and a LightCycler 480 System (Roche). Primer sequences are listed in Table S3.

All biological replicates of different genotypes (N = 3–9) were run in the same plate and run as duplicate technical replicates. Relative gene expression of each gonad was normalized to the expression of the housekeeping genes *Shda* and *Tbp* by the 2-ΔΔCt calculation method. Fold change in gene expression was obtained by dividing the normalized gene expression in gonads of a given genotype by the mean of the normalized gene expression in control gonads. Data are shown as means ± SEM. Statistical significance was assessed by Mann-Whitney U two-tailed test (GraphPad Prism 10.2.1). * indicates P value ≤ 0.05; ns indicates P value > 0.05.

Acknowledgments

We acknowledge the help from members of the Experimental Histpathology Platform, the PRISM Imaging Platform and the Animal house at iBV (Institut de Biologie Valrose, Université Côte d'Azur, CNRS, Inserm, iBV, France). We are grateful to members of the A. Schedl, M.C. Chaboissier and S. Nef groups for helpful discussions and to D. Wilhelm for critical reading of the manuscript. We are indebted to Dr. Chaponnier, Dr. Inoue, Pr. Morohashi, Dr. M. Vasseur-Cognet and Dr. Wilhelm for sharing mouse lines and reagents. This research was funded by Agence Nationale de la Recherche: ANR-19-CE14-0022, SexDiff and ANR-23-CE14-0012, Heterosex, and by a scholarship from the China Scholarship Council (to F.T.).

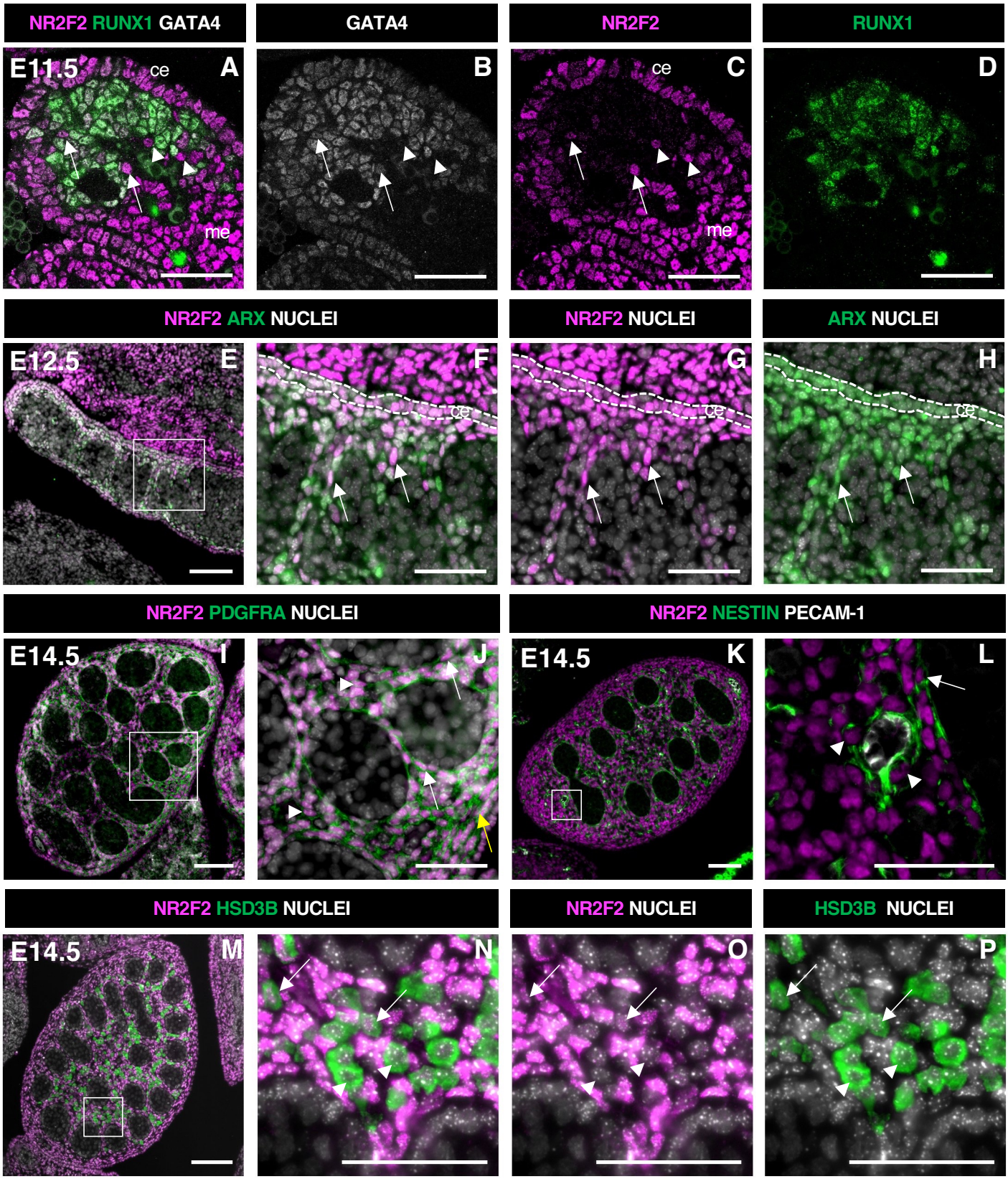
NR2F2 RUNX1 GATA4
GATA4
NR2F2
RUNX1
E11.5
ce
A
B
C
D
me
NR2F2 ARX NUCLEI
NR2F2 NUCLEI
ARX NUCLEI
E12.5
E
F
G
H
NR2F2 PDGFRA NUCLEI
NR2F2 NESTIN PECAM-1
E14.5
I
J
K
L
NR2F2 HSD3B NUCLEI
NR2F2 NUCLEI
HSD3B NUCLEI
M
N
O
P

Figure 1

Figure legends

Figure 1. NR2F2 is expressed in steroidogenic progenitors of the fetal testis

(A-D) Immunodetection of NR2F2, RUNX1 and GATA4 on E11.5 (18 tail somites) XY gonad. NR2F2 is detected in coelomic epithelium (ce), mesonephros (me) and RUNX1 negative cells that are either GATA4 positive (arrows in A-C) or GATA4 negative (arrowheads in A-C). **(E-H)** Immunodetection of NR2F2 and ARX on E12.5 XY gonad. NR2F2 is co-expressed with ARX in the coelomic epithelium (ce, dotted lines in F-H) and in interstitial cells between the testis cords (arrows in F-H). **(I,J)** Immunodetection of NR2F2 and PDGFRA on E14.5 XY gonad. NR2F2 is detected in PDGFRA positive cells including interstitial progenitors (arrowheads in J), peritubular myoid cell surrounding testis cords (arrows in J), and cells of the future tunica albuginea (yellow arrow in J). **(K,L)** Immunodetection of NR2F2, NESTIN and PECAM-1 on E14.5 XY gonad. NR2F2 is detected in NESTIN positive interstitial progenitors including perivascular cells (arrowheads in L) and peritubular myoid cells (arrow in L). **(M-P)** Immunodetection of NR2F2 and HSD3B on E14.5 XY gonad. NR2F2 is absent from the majority of HSD3B positive Fetal Leydig cells (arrowheads in N-P) and is only detected at low levels in few HSD3B positive elongated cells (arrows in N-P). Data are representative of triplicate biological replicates. Scale bar = 50 μm in A-D, F-H, J, L and N-P. Scale bar = 100 μm in E, I, K, M.

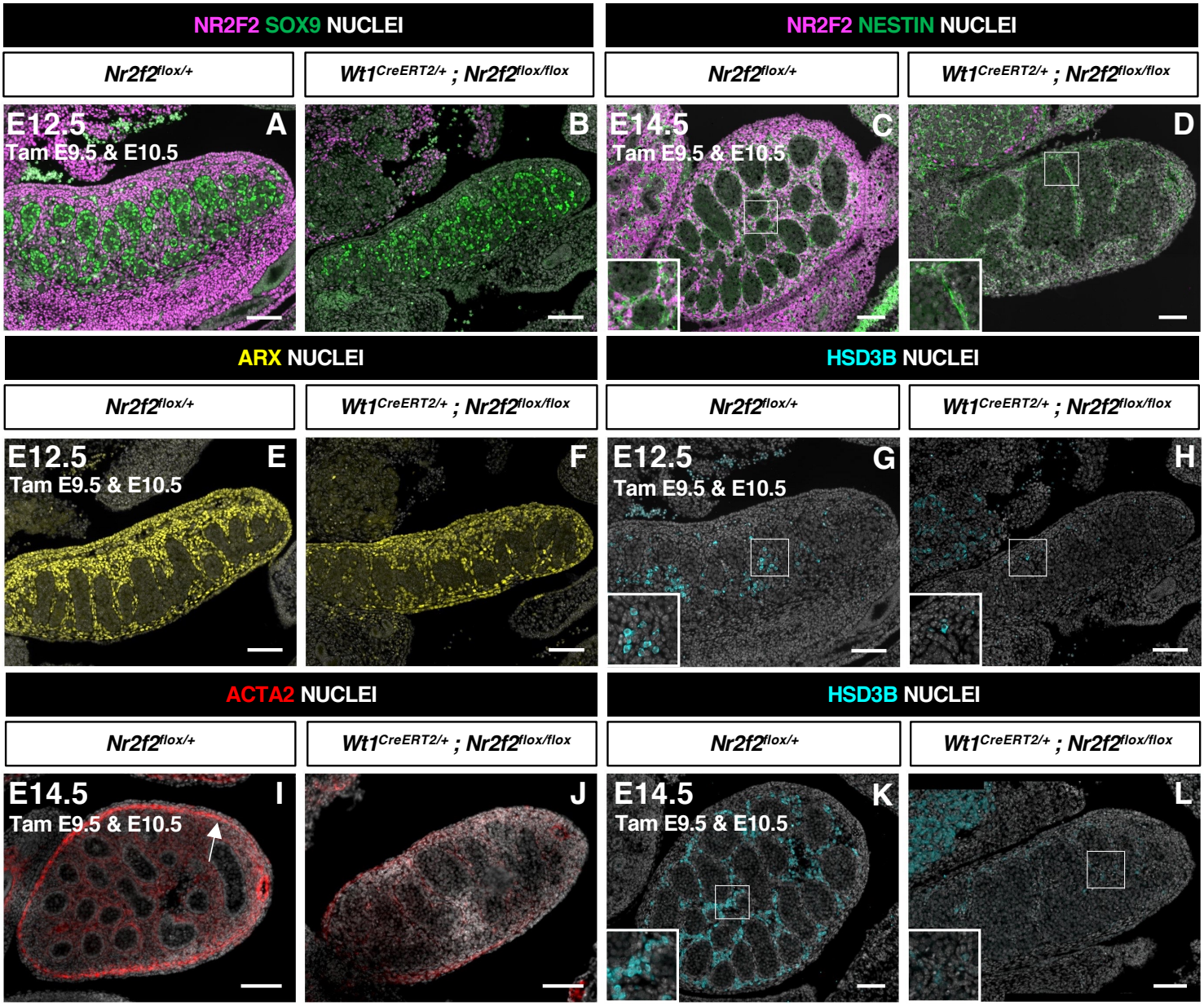
NR2F2 SOX9 NUCLEI
Nr2f2flox/+
Wt1CreERT2/+ ; Nr2f2flox/flox
E12.5
Tam E9.5 & E10.5
A
B
NR2F2 NESTIN NUCLEI
Nr2f2flox/+
Wt1CreERT2/+ ; Nr2f2flox/flox
E14.5
Tam E9.5 & E10.5
C
D
ARX NUCLEI
Nr2f2flox/+
Wt1CreERT2/+ ; Nr2f2flox/flox
E12.5
Tam E9.5 & E10.5
E
F
HSD3B NUCLEI
Nr2f2flox/+
Wt1CreERT2/+ ; Nr2f2flox/flox
E12.5
Tam E9.5 & E10.5
G
H
ACTA2 NUCLEI
Nr2f2flox/+
Wt1CreERT2/+ ; Nr2f2flox/flox
E14.5
Tam E9.5 & E10.5
I
J
HSD3B NUCLEI
Nr2f2flox/+
Wt1CreERT2/+ ; Nr2f2flox/flox
E14.5
Tam E9.5 & E10.5
K
L

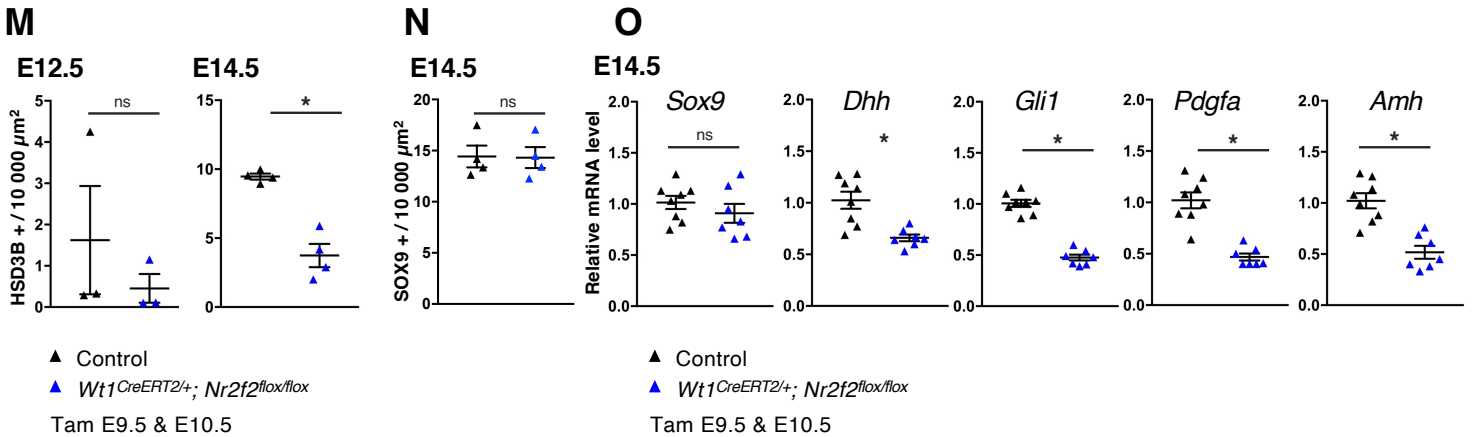
M
E12.5
E14.5
HSD3B + / 10 000 µm²
ns
*
N
E14.5
SOX9 + / 10 000 µm²
ns
O
E14.5
Relative mRNA level
Sox9
Dhh
Gli1
Pdgfa
Amh
ns
*
Control
Wt1CreERT2/+; Nr2f2flox/flox
Tam E9.5 & E10.5
Control
Wt1CreERT2/+; Nr2f2flox/flox
Tam E9.5 & E10.5

Figure 2

Figure 2. NR2F2 deletion by WT1^{CreERT2} impairs Sertoli cell differentiation and FLC development

(A,B) Immunodetection of NR2F2 and SOX9 on E12.5 control and *WT1^{CreERT2}; Nr2f2$^{flox/flox}$* testes after tamoxifen treatment at E9.5 and E10.5. NR2F2 is efficiently deleted in the gonad and mesonephros. **(C,D)** Immunodetection of NR2F2 and NESTIN on E14.5 control and *WT1^{CreERT2}; Nr2f2$^{flox/flox}$* testes. NR2F2 is efficiently deleted in NESTIN1 positive cells. **(E,F)** Immunodetection of ARX on E12.5 control and *WT1^{CreERT2}; Nr2f2$^{flox/flox}$* testes. Interstitial cells are generated in *WT1^{CreERT2}; Nr2f2$^{flox/flox}$* mutants. **(G,H)** Immunodetection of HSD3B on E12.5 control and *WT1^{CreERT2}; Nr2f2$^{flox/flox}$* testes. **(I,J)** Immunodetection of ACTA2 on E14.5 control and *WT1^{CreERT2}; Nr2f2$^{flox/flox}$* testes. The expression in the future tunica albuginea (arrow in I) is impaired in *WT1^{CreERT2}; Nr2f2$^{flox/flox}$* mutants. **(K,L)** Immunodetection of HSD3B on E14.5 control and *WT1^{CreERT2}; Nr2f2$^{flox/flox}$* testes. **(M)** Quantification of the number of HSD3B positive cells per surface unit in control and *WT1^{CreERT2}; Nr2f2$^{flox/flox}$* testes at E12.5 and E14.5. Each triangle represents the mean number of HSD3B or SOX9 positive cells per surface unit of one individual measured on at least two sections per gonad. Data are shown as means ± SEM. Statistical significance was assessed by Mann-Whitney U two-tailed test. * indicates P value ≤ 0.05; ns indicates P value > 0.05. **(N)** Quantification of the number of SOX9 positive cells per surface unit in control *WT1^{CreERT2}; Nr2f2$^{flox/flox}$* testes at E14.5. Each triangle rrepresents the mean number of SOX9 positive cells per surface unit of one individual measured on at least two sections per gonad. Data are shown as means ± SEM. Statistical significance was assessed by Mann-Whitney U two-tailed test. * indicates P value ≤ 0.05; ns indicates P value > 0.05. **(O)** Quantification of *Sox9, Dhh, Gli1, Pdgfa* and *Amh* transcripts after normalization to *Sdha* and *Tbp* by RT-qPCR at E14.5. Data are shown as means ± SEM. Statistical significance was assessed by Mann-Whitney U two-tailed test. * indicates P value ≤ 0.05; ns indicates P value > 0.05. Tamoxifen was administered at E9.5 and E10.5. Immunodetection data are representative of triplicate biological replicates. Scale bar = 100 µm.

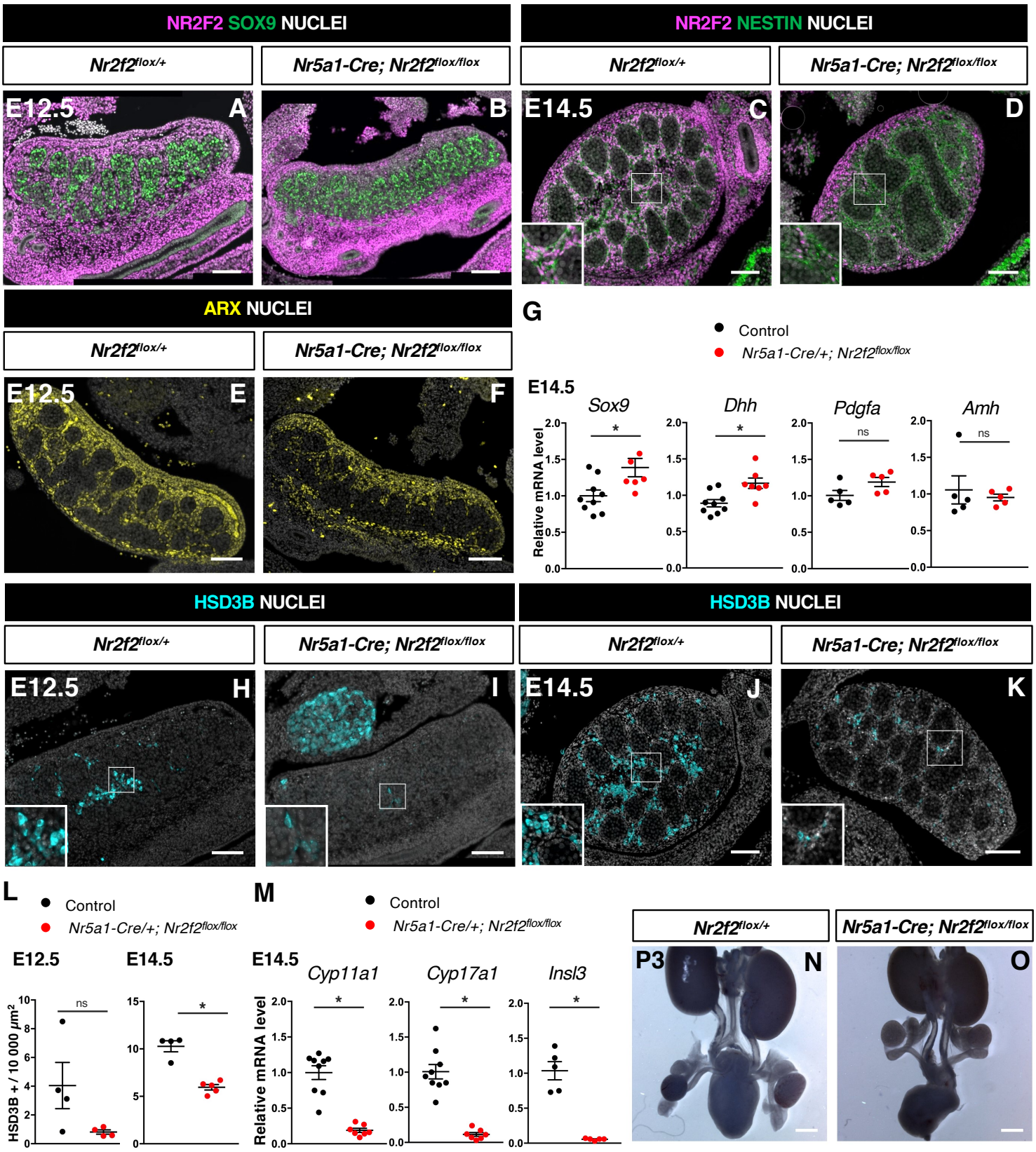
NR2F2 SOX9 NUCLEI
Nr2f2flox/+
Nr5a1-Cre; Nr2f2flox/flox
E12.5
A
B
NR2F2 NESTIN NUCLEI
E14.5
C
D
ARX NUCLEI
E
F
G
Control
Nr5a1-Cre/+; Nr2f2flox/flox
Sox9
Dhh
Pdgfa
Amh
Relative mRNA level
ns
HSD3B NUCLEI
H
I
J
K
L
HSD3B + / 10 000 µm²
M
Cyp11a1
Cyp17a1
Insl3
P3
N
O

Figure 3

Figure 3. NR2F2 deletion by Nr5a1-Cre impairs FLC development

(A,B) Immunodetection of NR2F2 and SOX9 on E12.5 control and *Nr5a1-Cre; Nr2f2*$^{flox/flox}$ testes. NR2F2 is deleted in interstitial cells but is still present in the outermost layer of the testis. **(C,D)** Immunodetection of NR2F2 and NESTIN on E14.5 control and *Nr5a1-Cre; Nr2f2*$^{flox/flox}$ testes. NR2F2 is still detected in NESTIN1 positive cells. **(E,F)** Immunodetection of ARX on E12.5 control and *Nr5a1-Cre; Nr2f2*$^{flox/flox}$ testes. Interstitial cells are generated in *Nr5a1-Cre; Nr2f2*$^{flox/flox}$ mutants. **(G))** Quantification of *Sox9, Dhh, Pdgfa* and *Amh* transcripts after normalization to *Sdha* and *Tbp* by RT-qPCR at E14.5. Data are shown as means ± SEM. Statistical significance was assessed by Mann-Whitney U two-tailed test. * indicates P value ≤ 0.05; ns indicates P value > 0.05. **(H,I)** Immunodetection of HSD3B on E12.5 control and *Nr5a1-Cre; Nr2f2*$^{flox/flox}$ testes. **(J,K)** Immunodetection of HSD3B on E14.5 control and *Nr5a1-Cre; Nr2f2*$^{flox/flox}$ testes. **(L)** Quantification of the number of HSD3B positive cells per surface unit in control and *Nr5a1-Cre; Nr2f2*$^{flox/flox}$ testes at E12.5 and E14.5. Each circle represents the mean number of HSD3B positive cells per surface unit of one individual measured on at least two sections per gonad. Data are shown as means ± SEM. Statistical significance was assessed by Mann-Whitney U two-tailed test. * indicates P value ≤ 0.05; ns indicates P value > 0.05. **(M)** Quantification of *Cyp11a1*, *Cyp17a1* and *Insl3* after normalization to *Sdha* and *Tbp* by RT-qPCR at E14.5. . Data are shown as means ± SEM. Statistical significance was assessed by Mann-Whitney U two-tailed test. * indicates P value ≤ 0.05; ns indicates P value > 0.05. **(N,O)** Macroscopic view of the urogenital tract of XY P3 control and *Nr5a1-Cre; Nr2f2*$^{flox/flox}$ mutants. The testes are in abdominal position in *Nr5a1-Cre; Nr2f2*$^{flox/flox}$ mutants. Immunodetection data are representative of triplicate biological replicates. Scale bar = 100 µm in A-F, H-K. Scale bar = 500 µm in N,O.

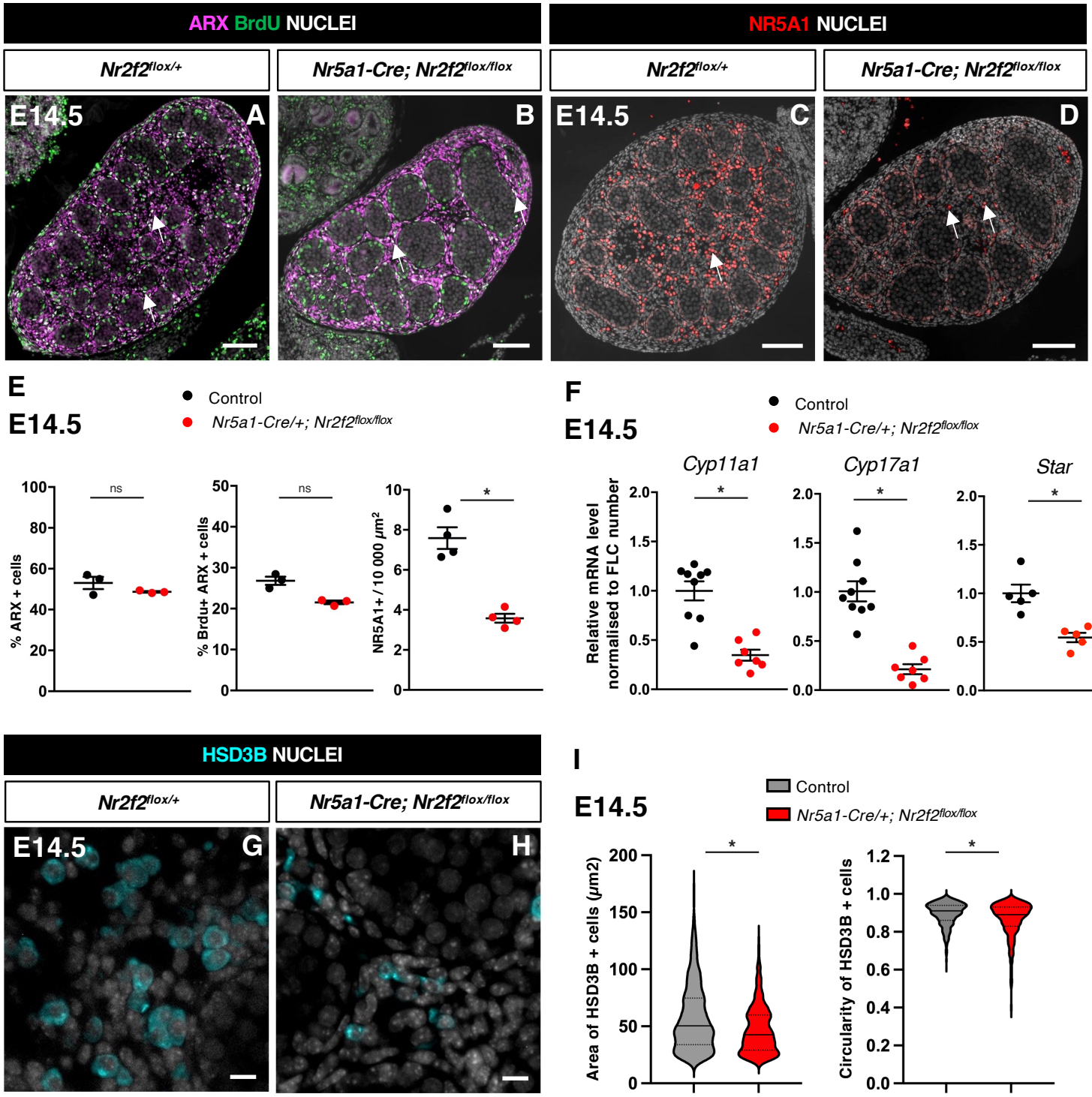
ARX BrdU NUCLEI
NR5A1 NUCLEI
Nr2f2flox/+
Nr5a1-Cre; Nr2f2flox/flox
Nr2f2flox/+
Nr5a1-Cre; Nr2f2flox/flox
E14.5
A
B
E14.5
C
D
E
E14.5
Control
Nr5a1-Cre/+; Nr2f2flox/flox
% ARX + cells
% Brdu+ ARX + cells
NR5A1+ / 10 000 µm2
ns
ns
*
F
E14.5
Control
Nr5a1-Cre/+; Nr2f2flox/flox
Cyp11a1
Cyp17a1
Star
Relative mRNA level normalised to FLC number
*
*
*
HSD3B NUCLEI
Nr2f2flox/+
Nr5a1-Cre; Nr2f2flox/flox
E14.5
G
H
I
E14.5
Control
Nr5a1-Cre/+; Nr2f2flox/flox
Area of HSD3B + cells (µm2)
Circularity of HSD3B + cells
*
*

Figure 4

Figure 4. NR2F2 function is required for the differentiation of steroidogenic progenitors

(A, B) Immunodetection of ARX, and BrdU (arrows) on E14.5 XY control and *Nr5a1-Cre; Nr2f2*$^{flox/flox}$ testes. (**C,D**) Immunodetection of NR5A1 on E14.5 XY control and *Nr5a1-Cre; Nr2f2*$^{flox/flox}$ testes. Arrows indicate strong expressing NR5A1 positive FLC. (**E)** Quantification of the percentage of ARX positive cells (number of ARX positive nuclei relative to the total number of nuclei labelled by DAPI), of the percentage of ARX positive cells labelled by BrdU (number of nuclei positive for ARX and BrdU relative to the number of ARX positive nuclei) and of the number of NR5A1 positive cells per surface unit in E14.5 XY control and *Nr5a1-Cre; Nr2f2*$^{flox/flox}$ testes. Each circle represents the mean percentage of ARX+ or ARX+/BrdU+ or NR5A1+ cells per surface unit of one individual measured on at least two sections per gonad. Data are shown as means ± SEM. Statistical significance was assessed by Mann-Whitney U two-tailed test. * indicates P value ≤ 0.05; ns indicates P value > 0.05. (**F**) RT-qPCR quantification of *Cyp11a1*, *Cyp17a1* and *Star* transcripts after normalization to *Sdha* and *Tbp* and to the number of FLC as quantified by HSD3B immunofluorescence at E14.5. Data are shown as means ± SEM. Statistical significance was assessed by Mann-Whitney U two-tailed test. * indicates P value ≤ 0.05; ns indicates P value > 0.05. (**G,H**) Immunodetection of HSD3B on E14.5 XY control and *Nr5a1-Cre; Nr2f2*$^{flox/flox}$ testes. (**I**) Quantification of the area and circularity of HSD3B positive cells in two E14.5 control (737 cells, grey violin plot) and three *Nr5a1-Cre; Nr2f2*$^{flox/flox}$ (486 cells, red violin plot) testes. Statistical significance was assessed by Mann-Whitney U two-tailed test. * indicates P value ≤ 0.05; ns indicates P value > 0.05. Immunodetection data are representative of triplicate biological replicates. Scale bar = 10 µm in G-H. Scale bar = 100 µm in A-D.

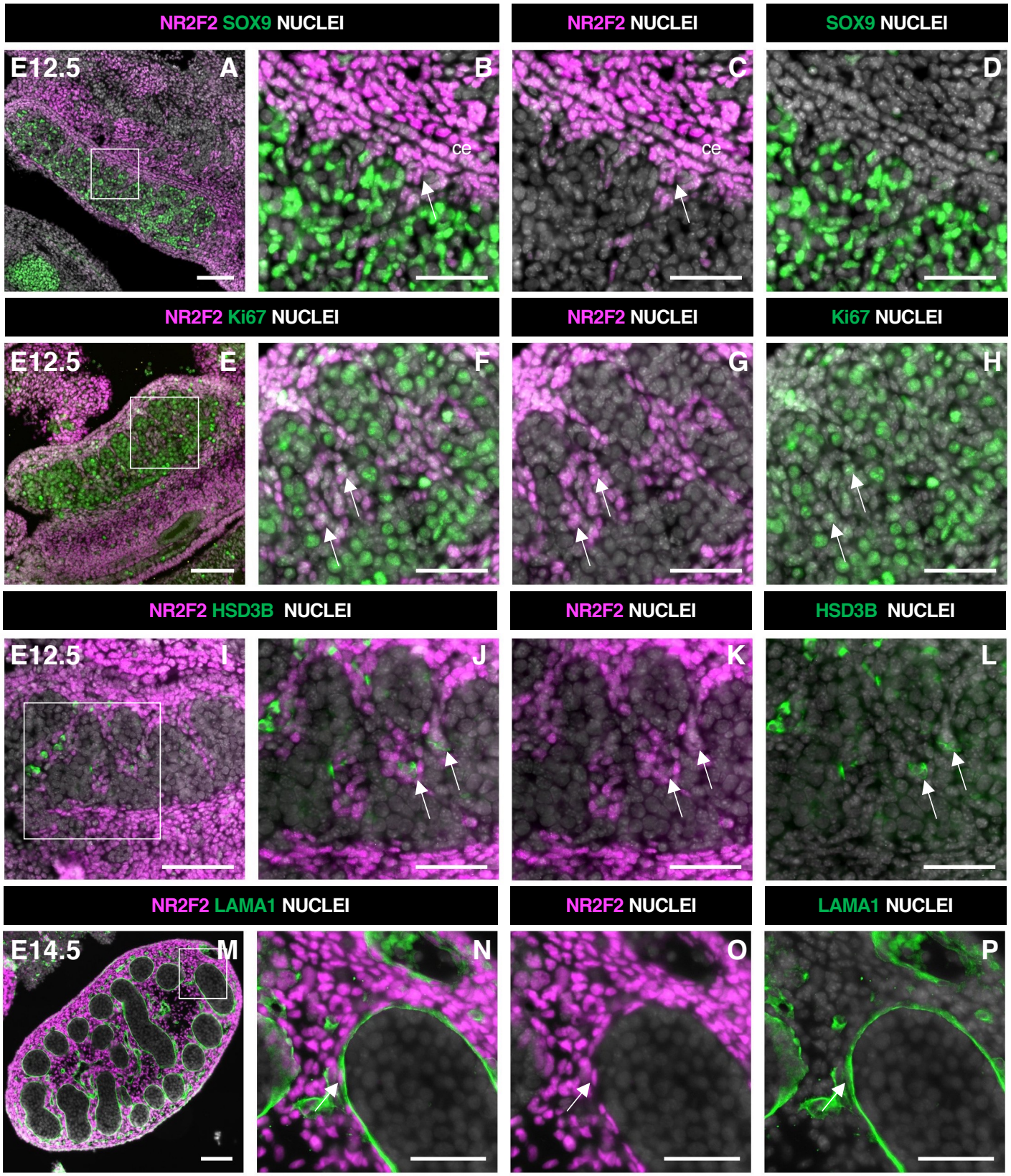
NR2F2 SOX9 NUCLEI
NR2F2 NUCLEI
SOX9 NUCLEI
E12.5
A
B
ce
C
ce
D
NR2F2 Ki67 NUCLEI
NR2F2 NUCLEI
Ki67 NUCLEI
E12.5
E
F
G
H
NR2F2 HSD3B NUCLEI
NR2F2 NUCLEI
HSD3B NUCLEI
E12.5
I
J
K
L
NR2F2 LAMA1 NUCLEI
NR2F2 NUCLEI
LAMA1 NUCLEI
E14.5
M
N
O
P

Figure S1

Figure S1. Relates to Figure1. NR2F2 is expressed in steroidogenic progenitors of the fetal testis

(A-D) Immunodetection of NR2F2, and SOX9 on E12.5 XY gonad. NR2F2 is detected in coelomic epithelium (ce) and in interstitial cells outside the testis cords (arrows in B and C). (**E-H)** Immunodetection of NR2F2 and Ki67 on E12.5 XY gonad. NR2F2 positive cells are proliferating (arrows in F-H). **(I-L)** Immunodetection of NR2F2 and HSD3B on E12.5 XY gonad. NR2F2 is detected at low levels in HSD3B positive elongated cells (arrows in J-L). **(M-P)** Immunodetection of NR2F2 and LAMA1 on E14.5 XY gonad. NR2F2 is expressed in peritubular myoid cells lining the basement membrane outside the testis cords (arrow in N-P). Data are representative of triplicate biological replicates. Scale bar = 50 μm in B-D, F-H, J-L and N-P. Scale bar = 100 μm in A, E, I, M.

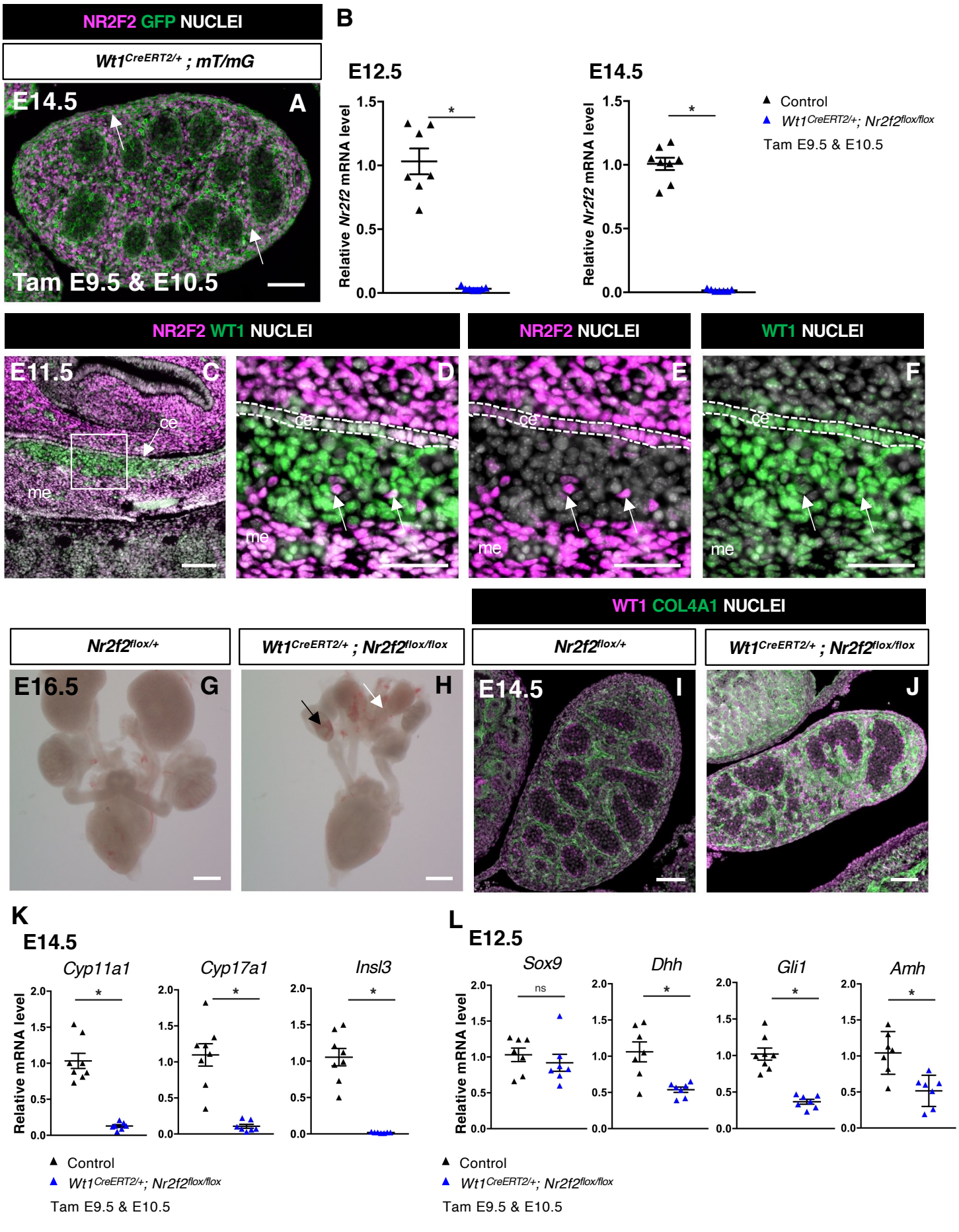
NR2F2 GFP NUCLEI
Wt1CreERT2/+ ; mT/mG
E14.5
A
Tam E9.5 & E10.5
B
E12.5
E14.5
Relative Nr2f2 mRNA level
Control
Wt1CreERT2/+; Nr2f2flox/flox
Tam E9.5 & E10.5
NR2F2 WT1 NUCLEI
NR2F2 NUCLEI
WT1 NUCLEI
E11.5
C
D
E
F
ce
me
WT1 COL4A1 NUCLEI
Nr2f2flox/+
Wt1CreERT2/+ ; Nr2f2flox/flox
E16.5
G
H
E14.5
I
J
K
E14.5
Cyp11a1
Cyp17a1
Insl3
Relative mRNA level
Control
Wt1CreERT2/+; Nr2f2flox/flox
Tam E9.5 & E10.5
L
E12.5
Sox9
Dhh
Gli1
Amh
ns
Relative mRNA level
Control
Wt1CreERT2/+; Nr2f2flox/flox
Tam E9.5 & E10.5

Figure S2

Figure S2. Relates to Figure 2. NR2F2 deletion by WT1^{CreERT2} impairs Sertoli cell differentiation and FLC development

(A) Immunodetection of NR2F2, and GFP on E14.5 XY *WT1^{CreERT2};mT/mG* gonad after tamoxifen was administered at E9.5 and E10.5. Upon Cre mediated recombination, GFP is expressed in all somatic cells of the gonad including NR2F2 positive cells (arrows). **(B)** Quantification of *Nr2f2* transcripts after normalization to *Sdha* and *Tbp* by RT-qPCR in control and *WT1^{CreERT2}; Nr2f2$^{flox/flox}$* testes dissected at E12.5 and E14.5 after tamoxifen treatment at E9.5 and E10.5. Data are shown as means ± SEM. Statistical significance was assessed by Mann-Whitney U two-tailed test. * indicates P value ≤ 0.05; ns indicates P value > 0.05. **(C-F)** Immunodetection of NR2F2 and WT1 on E11.5 XY gonad. NR2F2 is coexpressed with WT1 in the coelomic epithelium (ce), in the mesonephros (me), and in interstitial steroidogenic progenitors (arrows). **(G, H)** Macroscopic view of the urogenital tract of XY E16.5 control and *WT1^{CreERT2}; Nr2f2$^{flox/flox}$* testes dissected after tamoxifen treatment at E9.5 and E10.5. Testes (black arrow) and kidneys (white arrow) are hypoplastic in *WT1^{CreERT2}; Nr2f2$^{flox/flox}$* mutants. **(I,J)** Immunodetection of WT1 and COL4A1 on E14.5 control and *WT1^{CreERT2}; Nr2f2$^{flox/flox}$* testes. Testis cords are enlarged and abnormally shaped in *WT1^{CreERT2}; Nr2f2$^{flox/flox}$* mutants. **(K)** Quantification of *Cyp11a1*, *Cyp17a1* and *Insl3* transcripts after normalization to *Sdha* and *Tbp* by RT-qPCR at E14.5. **(L)** Quantification of *Sox9, Dhh, Gli1* and *Amh* transcripts after normalization to *Sdha* and *Tbp* by RT-qPCR at E12.5. Data are shown as means ± SEM. Statistical significance was assessed by Mann-Whitney U two-tailed test. * indicates P value ≤ 0.05; ns indicates P value > 0.05. Tamoxifen was administered at E9.5 and E10.5. Immunodetection data are representative of triplicate biological replicates. Scale bar = 50 µm in D-F. Scale bar = 100 µm in A, C, I, J. Scale bar = 500 µm in G, H.

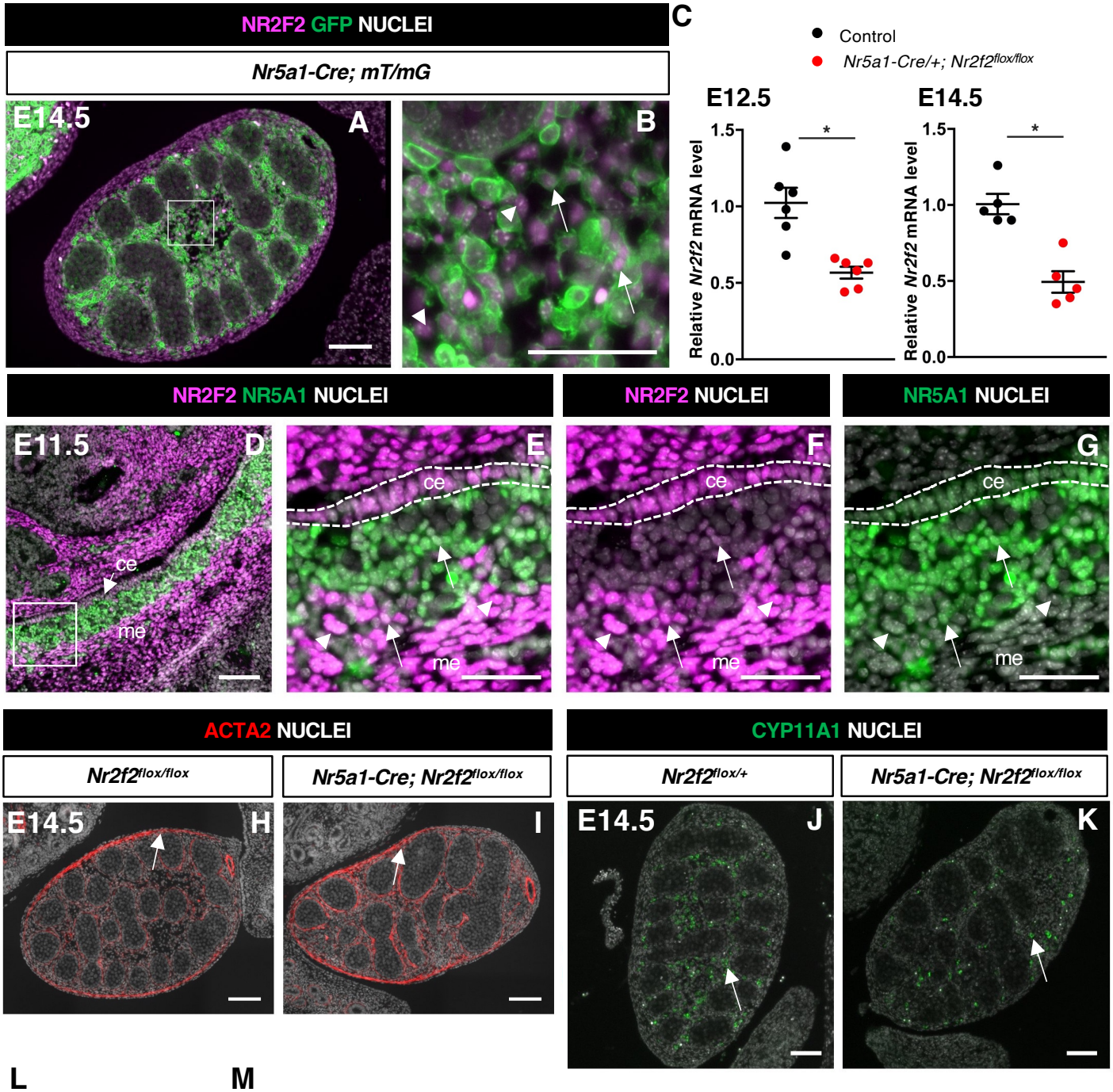
NR2F2 GFP NUCLEI
Nr5a1-Cre; mT/mG
E14.5
A
B
C
Control
Nr5a1-Cre/+; Nr2f2flox/flox
E12.5
E14.5
Relative Nr2f2 mRNA level
1.5
1.0
0.5
0.0
*
NR2F2 NR5A1 NUCLEI
NR2F2 NUCLEI
NR5A1 NUCLEI
E11.5
D
E
F
G
ce
me
ACTA2 NUCLEI
CYP11A1 NUCLEI
Nr2f2flox/flox
Nr5a1-Cre; Nr2f2flox/flox
Nr2f2flox/+
H
I
J
K

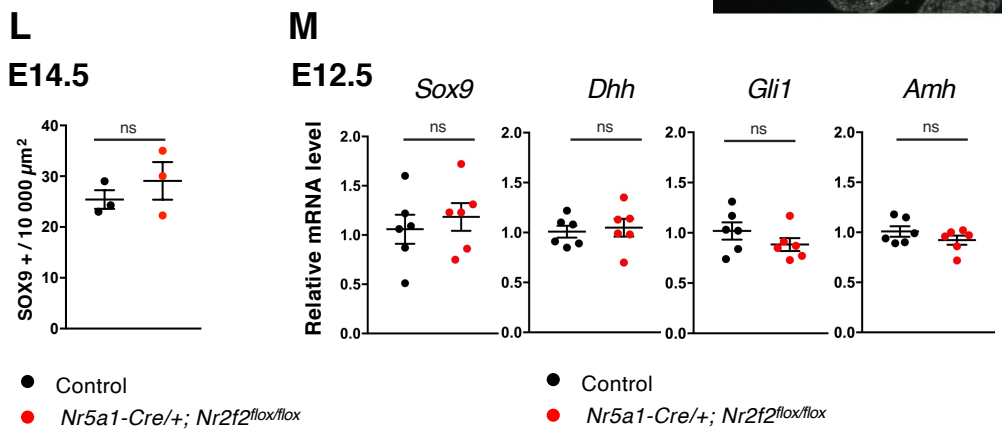
L
E14.5
SOX9 + / 10 000 µm²
40
30
20
10
0
ns
M
E12.5
Sox9
Dhh
Gli1
Amh
Relative mRNA level
2.0
1.5
1.0
0.5
0.0
ns
Control
Nr5a1-Cre/+; Nr2f2flox/flox

Figure S3

Figure S3. Relates to Figure 3. NR2F2 deletion by Nr5a1-Cre impairs FLC development

(A,B) Immunodetection of NR2F2, and GFP on E14.5 XY *Nr5a1-Cre;mT/mG* gonad. Upon Cre mediated recombination, GFP is expressed in somatic cells of the gonad including NR2F2 positive cells (arrows), however the outermost layer and some interstitial NR2F2 positive cells (arrowheads) do not express GFP. (**C)** Quantification of *Nr2f2* transcripts after normalization to *Sdha* and *Tbp* by RT-qPCR in control and *Nr5a1-Cre; Nr2f2*$^{flox/flox}$ testes dissected at E12.5 and E14.5. Data are shown as means ± SEM. Statistical significance was assessed by Mann-Whitney U two-tailed test. * indicates P value ≤ 0.05; ns indicates P value > 0.05. **(D-G)** Immunodetection of NR2F2 and NR5A1 on E11.5 XY gonad. NR2F2 is coexpressed with NR5A1 in the coelomic epithelium (ce) and in interstitial steroidogenic progenitors (arrows). NR2F2 positive cells that do not express NR5A1 are likely steroidogenic progenitors of mesonephric (me) origin (arrowheads). **(H, I)** Immunodetection of ACTA2 on E14.5 control and *Nr5a1-Cre; Nr2f2*$^{flox/flox}$ testes. White arrows indicate cells that will form the tunica albuginea. **(J,K)** Immunodetection of CYP11A1 (arrows) on E14.5 control and *Nr5a1-Cre; Nr2f2*$^{flox/flox}$ testes. **(L)** Quantification of the number of SOX9 positive cells per surface unit in control and *Nr5a1-Cre; Nr2f2*$^{flox/flox}$ testes at E14.5. Each circle represents the mean number of SOX9 positive cells per surface unit of one individual measured on at least two sections per gonad. Data are shown as means ± SEM. Statistical significance was assessed by Mann-Whitney U two-tailed test. * indicates P value ≤ 0.05; ns indicates P value > 0.05. **(M)** Quantification of *Sox9, Dhh, Gli1* and *Amh* transcripts after normalization to *Sdha* and *Tbp* by RT-qPCR at E12.5. Data are shown as means ± SEM. Statistical significance was assessed by Mann-Whitney U two-tailed test. * indicates P value ≤ 0.05; ns indicates P value > 0.05. Immunodetection data are representative of triplicate biological replicates. Scale bar = 50 μm in B, E-G. Scale bar = 100 μm in A, D, H, I, J, K.

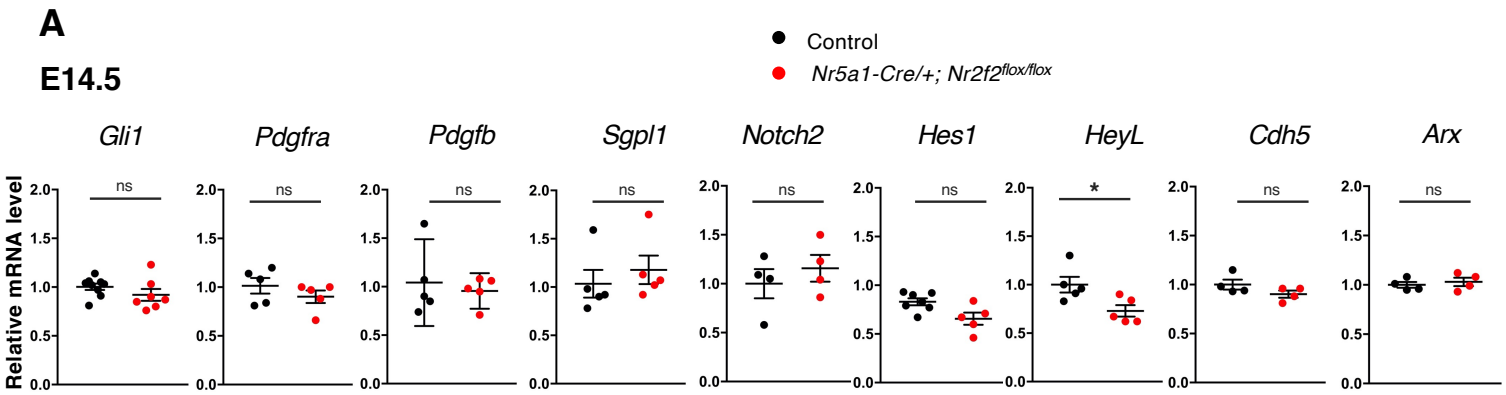
A
E14.5
Control
Nr5a1-Cre/+; Nr2f2flox/flox
Gli1
Pdgfra
Pdgfb
Sgpl1
Notch2
Hes1
HeyL
Cdh5
Arx
Relative mRNA level
ns
*

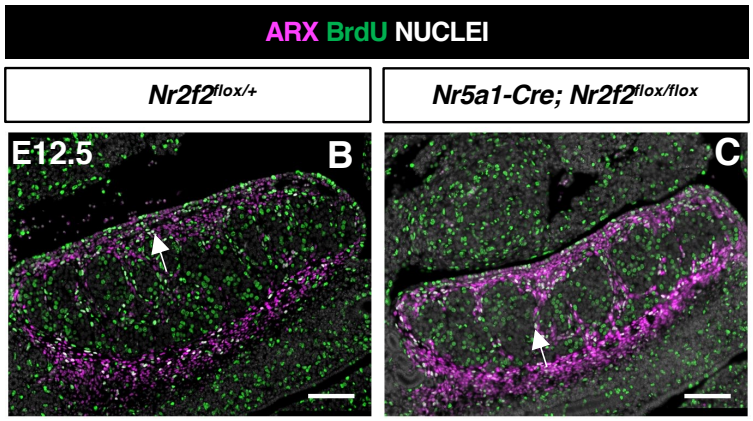
ARX BrdU NUCLEI
Nr2f2flox/+
Nr5a1-Cre; Nr2f2flox/flox
E12.5
B
C

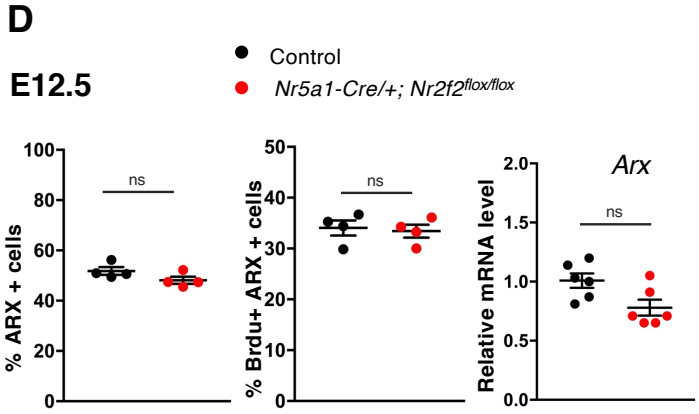
D
E12.5
Control
Nr5a1-Cre/+; Nr2f2flox/flox
% ARX + cells
% Brdu+ ARX + cells
Relative mRNA level
Arx
ns

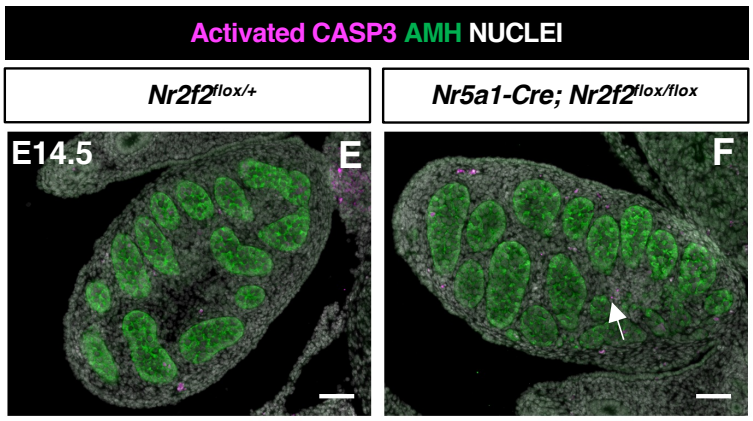
Activated CASP3 AMH NUCLEI
Nr2f2flox/+
Nr5a1-Cre; Nr2f2flox/flox
E14.5
E
F

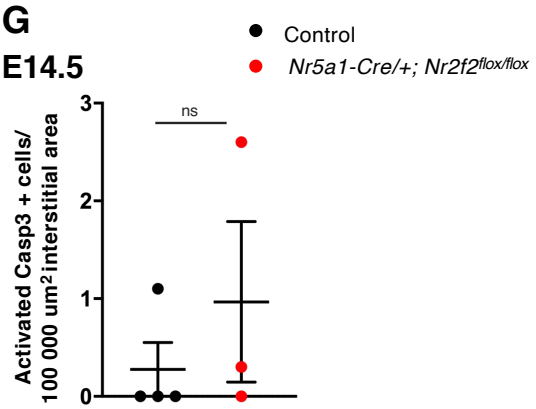
G
E14.5
Control
Nr5a1-Cre/+; Nr2f2flox/flox
Activated Casp3 + cells/
100 000 um2 interstitial area
ns

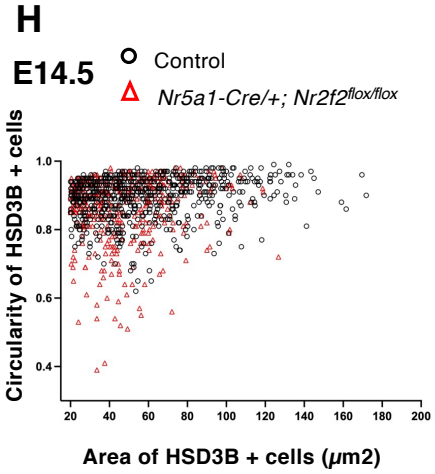
H
E14.5
Control
Nr5a1-Cre/+; Nr2f2flox/flox
Circularity of HSD3B + cells
Area of HSD3B + cells (μm2)

Figure S4

Figure S4. Relates to Figure 4. NR2F2 deletion by Nr5a1-Cre impairs FLC development

(A) Quantification of *Gli1*, *Pdgfra*, *Pdgfb* and *Sgpl1*, *Notch2, Hes1, HeyL, Cdh5* and *Arx* transcripts after normalization to *Sdha* and *Tbp* by RT-qPCR at E14.5. Statistical significance was assessed by Mann-Whitney U two-tailed test. * indicates P value ≤ 0.05; ns indicates P value > 0.05. **(B,C)** Immunodetection of ARX, and BrdU (arrows) on E12.5 XY control and *Nr5a1-Cre; Nr2f2*$^{flox/flox}$ testes. **(D)** Quantification of the percentage of ARX positive cells (number of ARX positive nuclei relative to the total number of nuclei labelled by DAPI) and of the percentage of ARX positive cells labelled by BrdU (number of nuclei positive for ARX and BrdU relative to the number of ARX positive nuclei) on E12.5 XY control and *Nr5a1-Cre; Nr2f2*$^{flox/flox}$ testes. Each circle represents the mean percentage of ARX+ or ARX+/BrdU+ cells per surface unit of one individual measured on at least two sections per gonad. Quantification of *Arx* transcripts after normalization to *Sdha* and *Tbp* by RT-qPCR at E12.5. Data are shown as means ± SEM. Statistical significance was assessed by Mann-Whitney U two-tailed test. ns indicates P value > 0.05. **(E,F)** Immunodetection of Activated Caspase3 (arrow in F) and AMH on E14.5 XY control and *Nr5a1-Cre; Nr2f2*$^{flox/flox}$ testes. **(G)** Quantification of the number of Caspase 3 positive cells per 100 000 μm^2 of interstitial area (area outside the testis cords) on E14.5 XY control and *Nr5a1-Cre; Nr2f2*$^{flox/flox}$ testes. Each circle represents the mean number of activated Caspase 3 positive cells per surface unit of one individual measured on at least two sections per gonad. Data are shown as means ± SEM. Statistical significance was assessed by Mann-Whitney U two-tailed test. ns indicates P value > 0.05. **(H)** Quantification of the circularity and area of HSD3B positive cells in two E14.5 control (737 cells, black open circles) and three *Nr5a1-Cre; Nr2f2*$^{flox/flox}$ (486 cells, red open triangles) testes. Immunodetection data are representative of triplicate biological replicates. Scale bar = 100 µm.

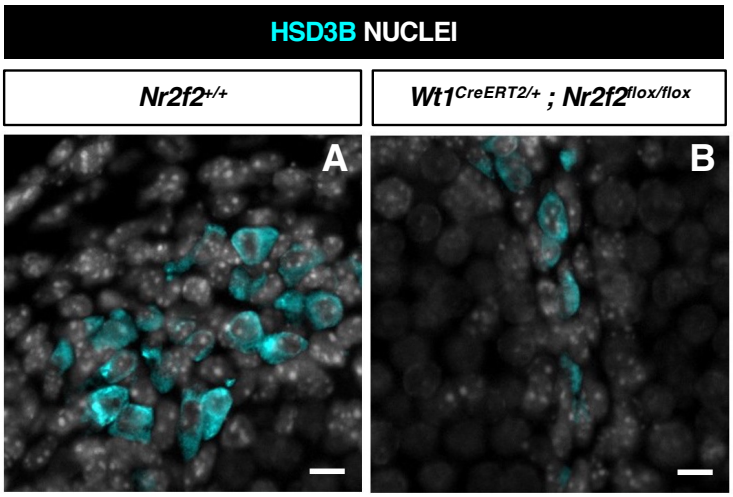
HSD3B NUCLEI
Nr2f2+/+
Wt1CreERT2/+ ; Nr2f2flox/flox
A
B

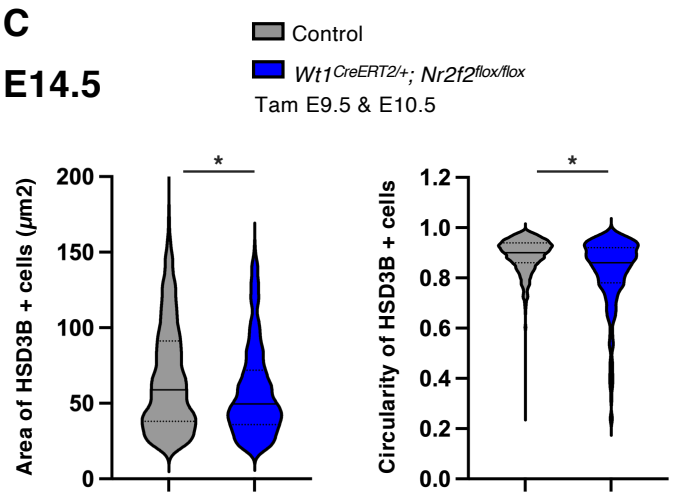
C
E14.5
Control
Wt1CreERT2/+; Nr2f2flox/flox
Tam E9.5 & E10.5
Area of HSD3B + cells (μm2)
Circularity of HSD3B + cells
*
*

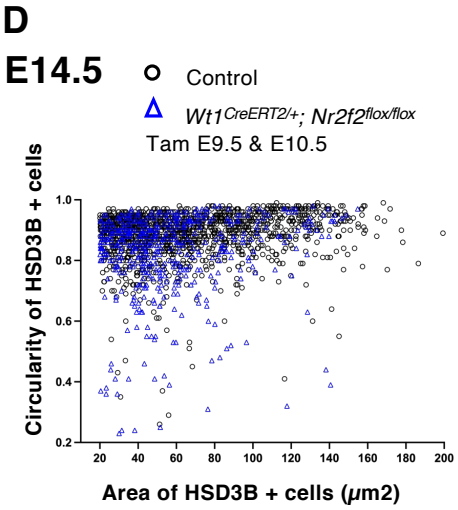
D
E14.5
Control
Wt1CreERT2/+; Nr2f2flox/flox
Tam E9.5 & E10.5
Circularity of HSD3B + cells
Area of HSD3B + cells (μm2)

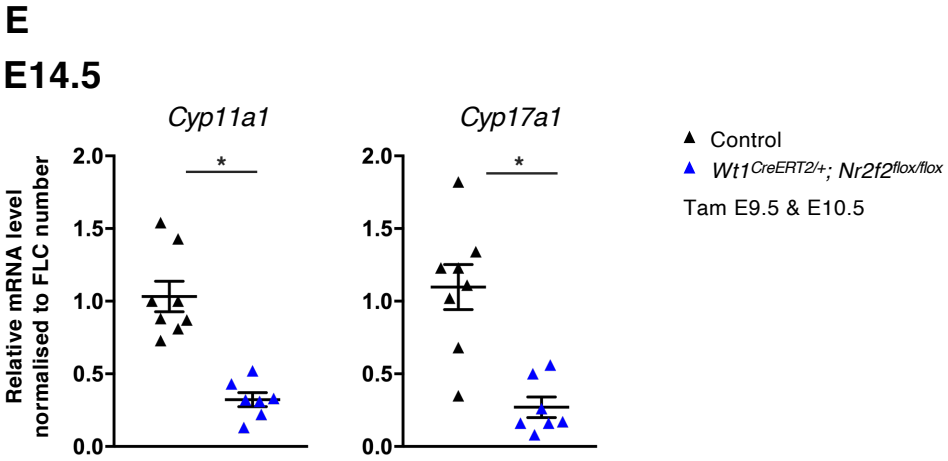
E
E14.5
Cyp11a1
Cyp17a1
Relative mRNA level normalised to FLC number
*
*
Control
Wt1CreERT2/+; Nr2f2flox/flox
Tam E9.5 & E10.5

Figure S5

Figure S5. Relates to Figure 4. NR2F2 deletion by *WT1^{CreERT2}* impairs FLC development

(**A,B**) Immunodetection of HSD3B on E14.5 XY control and *WT1^{CreERT2}; Nr2f2$^{flox/flox}$* testes. (**C**) Quantification of the area and circularity of HSD3B positive cells in three E14.5 control (1485 cells, grey violin plot) and three *WT1^{CreERT2}; Nr2f2$^{flox/flox}$* (474 cells, blue violin plot) testes. Statistical significance was assessed by Mann-Whitney U two-tailed test. * indicates P value ≤ 0.05; ns indicates P value > 0.05. **(D)** Quantification of the circularity and area of HSD3B positive cells in three E14.5 control (1485 cells, black open circles) and three *WT1^{CreERT2}; Nr2f2$^{flox/flox}$* (474 cells, blue open triangles) testes. (**E**) RT-qPCR quantification of *Cyp11a1* and *Cyp17a1* transcripts after normalization to *Sdha* and *Tbp* and to the number of FLC as quantified by HSD3B immunofluorescence at E14.5. Data are shown as means ± SEM. Statistical significance was assessed by Mann-Whitney U two-tailed test. * indicates P value ≤ 0.05; ns indicates P value > 0.05. Immunodetection data are representative of triplicate biological replicates. Scale bar = 10 μm in A-B.

Table S1: Genotyping primers

Primer name	Application	Sequence (5'- 3')
CRE 1	Genotyping *Cre*	CAGGATATACGTAATCTGGC
CRE 4	Genotyping *Cre*	CACGGGCACTGTGTCCAGACCAG
CCR5mR	Genotyping internal control	ATGTGGATGGAGAGGAGTCG
CCR5mL	Genotyping internal control	CAACCGAGACCTTCCTGTTC
TF2.1	Genotyping *Nr2f2*	TGCCCACACTTTCCTACTCC
TF2.5	Genotyping *Nr2f2*	TTTCTGCAAGGAATGGGTTG

5

Table S2: Antibodies

Antibody name	Raised in	Dilution	Source	Reference
ACTA2	mouse	1/500	Gift from Dr. Chaponnier	
Activated Caspase 3	rabbit	1/200	R&D Systems	AF835
AMH	mouse	1/50	Bio-Rad	MCA2246
ARX	rabbit	1/200	Gift from Pr. Morohashi and Dr. Inoue	
COL4A1	rabbit	1/400	Abcam	ab19808
CYP11A1	rabbit	1/200	Gift from Dr. Wilhelm	
GATA4	goat	1/200	Santa Cruz Biotechnology	Sc-1237
GFP	chicken	1/200	Abcam	ab13970
HSD3B	goat	1/200	Santa Cruz Biotechnology	Sc-30820
HSD3B	rabbit	1/500	Invitrogen	PA5-76669
Ki67	rabbit	1/200	Spring Bioscience	M3062
LAMA1	rabbit	1/200	Sigma-Aldrich	L9393
NESTIN	rabbit	1/1000	Biolegend	BL839801
NR2F2	mouse	1/200	R&D Systems	PP-H7147-00
NR5A1	rabbit	1/200	Cosmo Bio	KO611
PDGFRA	rabbit	1/200	Santa Cruz Biotechnology	SC-338
PECAM1	goat	1/200	Santa Cruz Biotechnology	Sc-1506
RUNX1	rabbit	1/500	Abcam	ab92336
SOX9	rabbit	1/250	Sigma-Aldrich	HPA001758
WT1	goat	1/200	R&D Systems	AF5729

Table S3: RT-qPCR primers

Primer name	Sequence (5'- 3')
Amh-Fwd	GGGGAGACTGGAGAACAGC
Amh-Rev	AGAGCTCGGGCTCCCATA
Arx-Fwd	GCACCACGTTCACCAGTTAC
Arx-Rev	GCACCACGTTCACCAGTTAC
Cdh5-Fwd	TCCTCTGCATCCTCACCATCACA
Cdh5-Rev	GTAAGTGACCAACTGCTCGTGAAT
Cyp11a1-Fwd	TGGCCCCATTTACAGGGAGAA
Cyp11a1-Rev	GGCATCTGAACTCTTAAACAGGA
Cyp17a1-Rev	CAGAGAAGTGCTCGTGAAGAAG
Cyp17a1Fwd	CAGAGAAGTGCTCGTGAAGAAG
Dhh-Fwd	GGACCTCGTACCCAACTACAA
Dhh-Rev	CGATGGCTAGAGCGTTCACC
Gli1-Fwd	TGGTACCATGAGCCCTTCTT
Gli1-Rev	GTGGTACACAGGGCTGGACT
Hes1-Fwd	ATAGCTCCCGGCATTCCAAG
Hes1-Rev	ATAGCTCCCGGCATTCCAAG
HeyL-Fwd	CAGCCCTTCGCAGATGCAA
HeyL-Rev	CCAATCGTCGCAATTCAGAAAG
Insl3-Fwd	ATTGCTCCCCACCTCCTGGCTATG
Insl3-Rev	GGTCATGATGGGGCTTCTTGGGGA
Notch2-Fwd	ATATCGACGACTGCCCCAAC
Notch2-Rev	CCATAGCCTCCGTTTCGGTT
Nr2f2-Fwd	CGGAGGAACCTGAGCTACAC
Nr2f2-Rev	CGGAGGAACCTGAGCTACAC
Pdgfa-Fwd	CAGTGTCAAGGTGGCCAAAGT
Pdgfa-Rev	CAGTGTCAAGGTGGCCAAAGT
Pdgfb-Fwd	GATCTCTCGGAACCTCATCG
Pdgfb-Rev	GATCTCTCGGAACCTCATCG
Pdgfra-Fwd	TCCATGCTAGACTCAGAAGTCA
Pdgfra-Rev	TCCCGGTGGACACAATTTTT
Sdha-Fwd	TGTTCAGTTCCACCCCACA
Sdha-Rev	TCTCCACGACACCCTTCTG
Sgpl1-Fwd	CTGAAGGACTTCGAGCCTTATTT
Sgpl1-Rev	CTGAAGGACTTCGAGCCTTATTT
Sox9-Fwd	GCGGAGCTCAGCAAGACTCTG
Sox9-Rev	ATCGGGGTGGTCTTTCTTGTG
Star-Fwd	AAGGCTGGAAGAAGGAAAGC
Star-Rev	CCACATCTGGCACCATCTTA
Tbp-Fwd	GCTCTGGAATTGTACCGCAG
Tbp-Rev	TGACTGCAGCAAATCGCTTG

References

1. A. P. Reyes, N. Y. León, E. R. Frost, V. R. Harley, Genetic control of typical and atypical sex development. *Nat Rev Urol* **20**, 434–451 (2023).

2. K. Miyabayashi, *et al.*, Alterations in Fetal Leydig Cell Gene Expression during Fetal and Adult Development. *Sex Dev* **11**, 53–63 (2017).

3. M. Inoue, *et al.*, Isolation and Characterization of Fetal Leydig Progenitor Cells of Male Mice. *Endocrinology* **157**, 1222–1233 (2016).

4. Y. Shima, *et al.*, Contribution of Leydig and Sertoli cells to testosterone production in mouse fetal testes. *Mol Endocrinol* **27**, 63–73 (2013).

5. H. Ademi, *et al.*, Deciphering the origins and fates of steroidogenic lineages in the mouse testis. *Cell Rep* **39**, 110935 (2022).

6. P. J. O'Shaughnessy, P. J. Baker, M. Heikkilä, S. Vainio, A. P. McMahon, Localization of 17beta-hydroxysteroid dehydrogenase/17-ketosteroid reductase isoform expression in the developing mouse testis--androstenedione is the major androgen secreted by fetal/neonatal leydig cells. *Endocrinology* **141**, 2631–2637 (2000).

7. S. Nef, L. F. Parada, Cryptorchidism in mice mutant for Insl3. *Nat Genet* **22**, 295–299 (1999).

8. S. Zimmermann, *et al.*, Targeted disruption of the Insl3 gene causes bilateral cryptorchidism. *Mol Endocrinol* **13**, 681–691 (1999).

9. J. M. Hutson, R. Li, B. R. Southwell, D. Newgreen, M. Cousinery, Regulation of testicular descent. *Pediatr Surg Int* **31**, 317–325 (2015).

10. Y. Shima, K.-I. Morohashi, Leydig progenitor cells in fetal testis. *Mol Cell Endocrinol* **445**, 55–64 (2017).

11. Y. Shima, Development of fetal and adult Leydig cells. *Reprod Med Biol* **18**, 323–330 (2019).

12. E. Rotgers, A. Jørgensen, H. H.-C. Yao, At the Crossroads of Fate-Somatic Cell Lineage Specification in the Fetal Gonad. *Endocr Rev* **39**, 739–759 (2018).

13. C. Mayère, *et al.*, Origin, specification and differentiation of a rare supporting-like lineage in the developing mouse gonad. *Sci Adv* **8**, eabm0972 (2022).

14. J. Karl, B. Capel, Sertoli cells of the mouse testis originate from the coelomic epithelium. *Dev Biol* **203**, 323–333 (1998).

15. I. Stévant, *et al.*, Deciphering Cell Lineage Specification during Male Sex Determination with Single-Cell RNA Sequencing. *Cell Rep* **22**, 1589–1599 (2018).

16. I. Stévant, *et al.*, Dissecting Cell Lineage Specification and Sex Fate Determination in Gonadal Somatic Cells Using Single-Cell Transcriptomics. *Cell Rep* **26**, 3272-3283.e3 (2019).

17. T. DeFalco, S. Takahashi, B. Capel, Two distinct origins for Leydig cell progenitors in the fetal testis. *Dev Biol* **352**, 14–26 (2011).

18. D. L. Kumar, T. DeFalco, A perivascular niche for multipotent progenitors in the fetal testis. *Nat Commun* **9**, 4519 (2018).

19. Q. Wen, C. Y. Cheng, Y.-X. Liu, Development, function and fate of fetal Leydig cells. *Semin Cell Dev Biol* **59**, 89–98 (2016).

20. H. H.-C. Yao, W. Whoriskey, B. Capel, Desert Hedgehog/Patched 1 signaling specifies fetal Leydig cell fate in testis organogenesis. *Genes Dev* **16**, 1433–1440 (2002).

21. I. Barsoum, H. H. C. Yao, Redundant and differential roles of transcription factors Gli1 and Gli2 in the development of mouse fetal Leydig cells. *Biol Reprod* **84**, 894–899 (2011).

22. I. B. Barsoum, N. C. Bingham, K. L. Parker, J. S. Jorgensen, H. H.-C. Yao, Activation of the Hedgehog pathway in the mouse fetal ovary leads to ectopic appearance of fetal Leydig cells and female pseudohermaphroditism. *Dev Biol* **329**, 96–103 (2009).

23. H. L. Park, *et al.*, Mouse Gli1 mutants are viable but have defects in SHH signaling in combination with a Gli2 mutation. *Development* **127**, 1593–1605 (2000).

24. A. Kothandapani, *et al.*, GLI3 resides at the intersection of hedgehog and androgen action to promote male sex differentiation. *PLoS Genet* **16**, e1008810 (2020).

25. F. Pierucci-Alves, A. M. Clark, L. D. Russell, A developmental study of the Desert hedgehog-null mouse testis. *Biol Reprod* **65**, 1392–1402 (2001).

26. A. M. Clark, K. K. Garland, L. D. Russell, Desert hedgehog (Dhh) gene is required in the mouse testis for formation of adult-type Leydig cells and normal development of peritubular cells and seminiferous tubules. *Biol Reprod* **63**, 1825–1838 (2000).

27. J. Brennan, C. Tilmann, B. Capel, Pdgfr-alpha mediates testis cord organization and fetal Leydig cell development in the XY gonad. *Genes Dev* **17**, 800–810 (2003).

28. M. Inoue, *et al.*, Tmsb10 triggers fetal Leydig differentiation by suppressing the RAS/ERK pathway. *Commun Biol* **5**, 974 (2022).

29. J. Schmahl, K. Rizzolo, P. Soriano, The PDGF signaling pathway controls multiple steroid-producing lineages. *Genes Dev* **22**, 3255–3267 (2008).

30. H. Tang, *et al.*, Notch signaling maintains Leydig progenitor cells in the mouse testis. *Development* **135**, 3745–3753 (2008).

31. C. Liu, K. Rodriguez, H. H.-C. Yao, Mapping lineage progression of somatic progenitor cells in the mouse fetal testis. *Development* **143**, 3700–3710 (2016).

32. T. Defalco, A. Saraswathula, A. Briot, M. L. Iruela-Arispe, B. Capel, Testosterone levels influence mouse fetal Leydig cell progenitors through notch signaling. *Biol Reprod* **88**, 91 (2013).

33. K.-I. Morohashi, M. Inoue, T. Baba, Coordination of Multiple Cellular Processes by NR5A1/Nr5a1. *Endocrinol Metab (Seoul)* **35**, 756–764 (2020).

34. T. Baba, *et al.*, Ad4BP/SF-1 regulates cholesterol synthesis to boost the production of steroids. *Commun Biol* **1**, 18 (2018).

35. T. Baba, *et al.*, Glycolytic genes are targets of the nuclear receptor Ad4BP/SF-1. *Nat Commun* **5**, 3634 (2014).

36. Y. Shima, *et al.*, Fetal Leydig cells dedifferentiate and serve as adult Leydig stem cells. *Development* **145**, dev169136 (2018).

37. M. B. Padua, *et al.*, Combined loss of the GATA4 and GATA6 transcription factors in male mice disrupts testicular development and confers adrenal-like function in the testes. *Endocrinology* **156**, 1873–1886 (2015).

38. M. Bielinska, A. Seehra, J. Toppari, M. Heikinheimo, D. B. Wilson, GATA-4 is required for sex steroidogenic cell development in the fetal mouse. *Dev Dyn* **236**, 203–213 (2007).

39. R. S. Viger, K. de Mattos, J. J. Tremblay, Insights Into the Roles of GATA Factors in Mammalian Testis Development and the Control of Fetal Testis Gene Expression. *Front Endocrinol (Lausanne)* **13**, 902198 (2022).

40. K. Miyabayashi, *et al.*, Aristaless related homeobox gene, Arx, is implicated in mouse fetal Leydig cell differentiation possibly through expressing in the progenitor cells. *PLoS One* **8**, e68050 (2013).

41. S.-Y. Li, *et al.*, Loss of Mafb and Maf distorts myeloid cell ratios and disrupts fetal mouse testis vascularization and organogenesis†. *Biol Reprod* **105**, 958–975 (2021).

42. S. Cui, *et al.*, Disrupted gonadogenesis and male-to-female sex reversal in Pod1 knockout mice. *Development* **131**, 4095–4105 (2004).

43. C. A. Schnabel, L. Selleri, M. L. Cleary, Pbx1 is essential for adrenal development and urogenital differentiation. *Genesis* **37**, 123–130 (2003).

44. S. Polvani, S. Pepe, S. Milani, A. Galli, COUP-TFII in Health and Disease. *Cells* **9**, 101 (2019).

45. F. A. Pereira, Y. Qiu, G. Zhou, M. J. Tsai, S. Y. Tsai, The orphan nuclear receptor COUP-TFII is required for angiogenesis and heart development. *Genes Dev* **13**, 1037–1049 (1999).

46. R. E. Mendoza-Villarroel, N. M. Robert, L. J. Martin, C. Brousseau, J. J. Tremblay, The nuclear receptor NR2F2 activates star expression and steroidogenesis in mouse MA-10 and MLTC-1 Leydig cells. *Biol Reprod* **91**, 26 (2014).

47. K. R. Kilcoyne, *et al.*, Fetal programming of adult Leydig cell function by androgenic effects on stem/progenitor cells. *Proc Natl Acad Sci U S A* **111**, E1924-1932 (2014).

48. S. van den Driesche, *et al.*, Proposed role for COUP-TFII in regulating fetal Leydig cell steroidogenesis, perturbation of which leads to masculinization disorders in rodents. *PLoS One* **7**, e37064 (2012).

49. G. Lottrup, *et al.*, Expression patterns of DLK1 and INSL3 identify stages of Leydig cell differentiation during normal development and in testicular pathologies, including testicular cancer and Klinefelter syndrome. *Hum Reprod* **29**, 1637–1650 (2014).

50. J. Qin, M.-J. Tsai, S. Y. Tsai, Essential roles of COUP-TFII in Leydig cell differentiation and male fertility. *PLoS One* **3**, e3285 (2008).

51. J. Taelman, *et al.*, Characterization of the human fetal gonad and reproductive tract by single-cell transcriptomics. *Dev Cell* **59**, 529-544.e5 (2024).

52. H. Zidoune, *et al.*, Novel Genomic Variants, Atypical Phenotypes and Evidence of a Digenic/Oligogenic Contribution to Disorders/Differences of Sex Development in a Large North African Cohort. *Front Genet* **13**, 900574 (2022).

53. M. Ganapathi, *et al.*, Heterozygous rare variants in NR2F2 cause a recognizable multiple congenital anomaly syndrome with developmental delays. *Eur J Hum Genet* **31**, 1117–1124 (2023).

54. C. M. Amato, H. H.-C. Yao, F. Zhao, One Tool for Many Jobs: Divergent and Conserved Actions of Androgen Signaling in Male Internal Reproductive Tract and External Genitalia. *Front Endocrinol (Lausanne)* **13**, 910964 (2022).

55. B. Nicol, *et al.*, RUNX1 maintains the identity of the fetal ovary through an interplay with FOXL2. *Nat Commun* **10**, 5116 (2019).

56. P. Bardoux, *et al.*, Essential role of chicken ovalbumin upstream promoter-transcription factor II in insulin secretion and insulin sensitivity revealed by conditional gene knockout. *Diabetes* **54**, 1357–63 (2005).

57. B. Zhou, *et al.*, Epicardial progenitors contribute to the cardiomyocyte lineage in the developing heart. *Nature* **454**, 109–113 (2008).

58. J. F. Armstrong, K. Pritchard-Jones, W. A. Bickmore, N. D. Hastie, J. B. Bard, The expression of the Wilms' tumour gene, WT1, in the developing mammalian embryo. *Mech Dev* **40**, 85–97 (1993).

59. N. L. Manuylov, F. O. Smagulova, L. Leach, S. G. Tevosian, Ovarian development in mice requires the GATA4-FOG2 transcription complex. *Development* **135**, 3731–3743 (2008).

60. C.-T. Yu, *et al.*, COUP-TFII is essential for metanephric mesenchyme formation and kidney precursor cell survival. *Development* **139**, 2330–2339 (2012).

61. N. C. Bingham, S. Verma-Kurvari, L. F. Parada, K. L. Parker, Development of a steroidogenic factor 1/Cre transgenic mouse line. *Genesis* **44**, 419–424 (2006).

62. N. L. Manuylov, *et al.*, Conditional ablation of Gata4 and Fog2 genes in mice reveals their distinct roles in mammalian sexual differentiation. *Dev Biol* **353**, 229–241 (2011).

63. S. G. Haider, Cell biology of Leydig cells in the testis. *Int Rev Cytol* **233**, 181–241 (2004).

64. P. Jeyasuria, *et al.*, Cell-Specific Knockout of Steroidogenic Factor 1 Reveals Its Essential Roles in Gonadal Function. *Molecular Endocrinology* **18**, 1610–1619 (2004).

65. F. W. Buaas, J. R. Gardiner, S. Clayton, P. Val, A. Swain, In vivo evidence for the crucial role of SF1 in steroid-producing cells of the testis, ovary and adrenal gland. *Development* **139**, 4561–4570 (2012).

66. P. Sararols, *et al.*, Specific Transcriptomic Signatures and Dual Regulation of Steroidogenesis Between Fetal and Adult Mouse Leydig Cells. *Front Cell Dev Biol* **9**, 695546 (2021).

67. S. Mehanovic, *et al.*, Identification of novel genes and pathways regulated by the orphan nuclear receptor COUP-TFII in mouse MA-10 Leydig cells†. *Biol Reprod* **105**, 1283–1306 (2021).

68. S. Mehanovic, K. J. Pierre, R. S. Viger, J. J. Tremblay, Chicken ovalbumin upstream promoter transcription factor type II interacts and functionally cooperates with GATA4 to regulate anti-Müllerian hormone receptor type 2 transcription in mouse MA-10 Leydig cells. *Andrology* **10**, 1411–1425 (2022).

69. M. Di-Luoffo, K. J. Pierre, N. M. Robert, M.-J. Girard, J. J. Tremblay, The nuclear receptors SF1 and COUP-TFII cooperate on the Insl3 promoter in Leydig cells. *Reproduction* **164**, 31–40 (2022).

70. R. E. Mendoza-Villarroel, *et al.*, The INSL3 gene is a direct target for the orphan nuclear receptor, COUP-TFII, in Leydig cells. *J Mol Endocrinol* **53**, 43–55 (2014).

71. J. Cool, T. DeFalco, B. Capel, Testis formation in the fetal mouse: dynamic and complex de novo tubulogenesis. *Wiley Interdiscip Rev Dev Biol* **1**, 847–859 (2012).

72. A. Bashamboo, *et al.*, Loss of Function of the Nuclear Receptor NR2F2, Encoding COUP-TF2, Causes Testis Development and Cardiac Defects in 46,XX Children. *Am J Hum Genet* **102**, 487–493 (2018).

73. F. Tang, N. Richardson, A. Albina, M.-C. Chaboissier, A. Perea-Gomez, Mouse Gonad Development in the Absence of the Pro-Ovary Factor WNT4 and the Pro-Testis Factor SOX9. *Cells* **9** (2020).